ACADEMIC PRESS

Available online at www.sciencedirect.com

SCIENCE DIRECT®

Journal of Sound and Vibration 267 (2003) 809–850

JOURNAL OF SOUND AND VIBRATION

www.elsevier.com/locate/jsvi

Vibration sensitive behaviour of a connecting angle. Case of coupled beams and plates

M. Ouisse*, J.L. Guyader

Laboratoire Vibrations Acoustique, INSA Lyon-Batiment St Exupery, 25 bis, avenue Jean Capelle, 69621 Villeurbanne Cedex, France

Received 10 April 2002; accepted 14 October 2002

Abstract

In this paper semi-infinite one- and two-dimensional (1-D and 2-D) coupled structures are considered in order to find conditions under which coupling effects can induce hypersensitive vibrating behaviour. The approach is based on classical wave decomposition, and the first point is to show that high sensitivity can exist in such simple systems. Then, for the case of beams, it is shown that two critical coupling angles can be defined, and that their values depend only on wave number ratio. A similar study is then performed on semi-infinite coupled plates, and the existence of a critical coupling angle is shown. Its value can be determined using three structural parameters. The results are finally compared to finite coupled structures.

1. Introduction

Uncertainty can be a major questioning source as soon as manufacturing processes are used to build structures. Many reports have been presented [1,2], in which people show that sensitivity causes can be numerous in complex systems, and are not easily detectable. In our recent work [3], a method that could help one to predict which structural zones are responsible for hypersensitive behaviour [4] has been presented. In Refs. [4,5], a study concerning coupled plates has been used to show that a small shift of coupling angle could induce very large variations of response, when the nominal coupling angle has a particular value. This value depends on the characteristics of the structure, and has been determined for only a few specific cases. In the present paper a basic study is presented to find values of coupling angles which are in many cases responsible for vibration sensitive behaviour. This work is based on a wave approach in semi-infinite coupled structures

*Corresponding author. Tel.: +33-472-436-215; fax: +33-472-438-712.
E-mail address: ouisse@lva.insa-lyon.fr (M. Ouisse).

0022-460X/03/$ - see front matter
doi:10.1016/S0022-460X(03)00179-2

(coupled beams and coupled plates), in order that the number of structural parameters remains low.

The first part deals with semi-infinite coupled beams. Wave approaches for this kind of structure are well-developed, because of their simplicity, and their use is common in the field of joints between structures. Horner and White [6] have presented equations corresponding to coupling effects between bending and in-plane movements due to connecting angle, in terms of transmitted and reflected powers. They show that for particular joint angle values, transmitted or reflected power could be very sensitive to this angle. Guo [7] has shown results for models of joint behaviour, using masses and stiffnesses. Even if its results are not interpreted in terms of sensitivity, the equations that he developed are used here to find the conditions under which the coupled structure is sensitive. These conditions are derived using a single structural parameter, and linked to results concerning eigenvalues sensitivities of finite coupled beams.

The second part is comparable to the previous one, except that the structures are semi-infinite coupled plates. Coupling effects have been described by Langley and Heron [8], while sensitive behaviour has been observed for in-plane waves by Kil et al. [9] for small values of joint angle. Even if the structural parameters are more numerous than coupled beams cases, the conditions under which coupled plates can have sensitive behaviour are described in this paper and linked to the response variability of finite plates.

2. Study of two coupled semi-infinite beams

The considered structure is built with two coupled semi-infinite identical beams, presented in Fig. 1. Constitutive materials are supposed to be homogeneous and isotropic, and Bernoulli's formulation is used to describe the vibrating behaviour of the structure. Both bending and longitudinal movements are considered, and are not independent because of the coupling angle α. Bending movements are belonging to $(O, \vec{x_1}, \vec{y_1})$ plane, longitudinal displacements are along $(O, \vec{x_1})$ and $(O, \vec{x_2})$ axis, while coupling point is O.

The notations used for the forced waves decomposition are detailed in Appendix E.

bending movement:

- Beam number 1 (corresponding to $x_1 < 0$) is supposed to be the one in which there is an incident bending wave of unit amplitude, travelling toward the coupling point:

$$w_i(x_1) = \mathrm{e}^{-\mathrm{j}kx_1}, \tag{1}$$

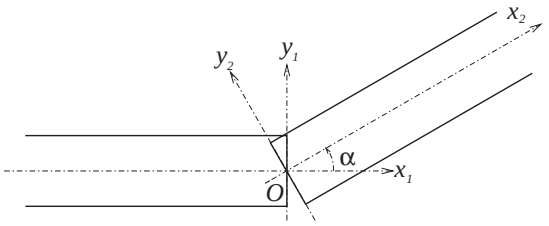

Fig. 1. Two coupled semi-infinite beams.

where $j^2 = 1$ and $k = \sqrt{\omega}(\rho S/EI)^{1/4}$ is the bending wave number of the beam. One should note that this choice of unit amplitude will bring large values of quantities if they are interpreted as MKS values, that is why units corresponding to displacements and powers are not labelled in figures.

Another wave exists in this beam, because of reflection effects on the coupling line. One can distinguish its evanescent and propagative parts:

$$w_r(x_1) = Ae^{kx_1} + Be^{jkx_1}, \tag{2}$$

where A and B are not known.

- Beam number 2 ($x_2 > 0$) movement is imposed by the coupling. Then, the transmitted bending wave can be written as

$$w_t(x_2) = Ce^{-kx_2} + De^{-jkx_2}, \tag{3}$$

where C and D are not known.

As far as longitudinal vibrations are concerned:

- In beam 1 a travelling reflected longitudinal wave is generated by coupling effects:

$$u_r(x_1) = Fe^{j\lambda x_1}, \tag{4}$$

in which F is unknown and $\lambda = \omega\sqrt{\rho/E}$ is the longitudinal wave number of the beam.

- In beam 2, a transmitted travelling wave is generated by the coupling:

$$u_t(x_2) = Ge^{-j\lambda x_2}, \tag{5}$$

where G is not known.

2.1. Equations

Once displacements fields are known, the generalized forces can be determined using constitutive laws linking forces and displacement fields, which can be written for the bending moment M, shear force T and longitudinal force N:

$$M(x) = EI\frac{d^2w}{dx^2}, \tag{6}$$

$$T(x) = -EI\frac{d^3w}{dx^3}, \tag{7}$$

$$N(x) = ES\frac{du}{dx}. \tag{8}$$

These relations are valid if they are used to define cohesion forces corresponding to an external normal oriented toward increasing x. It is also possible to define the rotation of the beam cross-section:

$$\Omega(x) = \frac{dw}{dx}. \tag{9}$$

Then, one can determine each of the six unknowns, using continuity equations at the coupling point $x = 0$:

- Displacement continuity:

$$w_t(0) = (w_i(0) + w_r(0))\cos\alpha + u_r(0)\sin\alpha, \tag{10}$$

$$u_t(0) = -(w_i(0) + w_r(0))\sin\alpha + u_r(0)\cos\alpha. \tag{11}$$

- Rotation continuity:

$$\frac{\mathrm{d}w_t}{\mathrm{d}x_2}(0) = \frac{\mathrm{d}(w_i + w_r)}{\mathrm{d}x_1}(0). \tag{12}$$

- Bending moment continuity:

$$EI\frac{\mathrm{d}^2 w_t}{\mathrm{d}x_2^2}(0) = EI\frac{\mathrm{d}^2(w_i + w_r)}{\mathrm{d}x_1^2}(0). \tag{13}$$

- Shear and normal forces continuity:

$$-EI\frac{\mathrm{d}^3 w_t}{\mathrm{d}x_2^3}(0) = -EI\frac{\mathrm{d}^3(w_i + w_r)}{\mathrm{d}x_1^3}(0)\cos\alpha + ES\frac{\mathrm{d}u_r}{\mathrm{d}x_1}(0)\sin\alpha, \tag{14}$$

$$ES\frac{\mathrm{d}u_t}{\mathrm{d}x_2}(0) = EI\frac{\mathrm{d}^3(w_i + w_r)}{\mathrm{d}x_1^3}(0)\sin\alpha + ES\frac{\mathrm{d}u_r}{\mathrm{d}x_1}(0)\cos\alpha. \tag{15}$$

These six equations can be written in the following forms:

$$\begin{bmatrix} \cos\alpha & \cos\alpha & -1 & -1 & \sin\alpha & 0 \\ \sin\alpha & \sin\alpha & 0 & 0 & -\cos\alpha & 1 \\ 1 & \mathrm{j} & 1 & \mathrm{j} & 0 & 0 \\ 1 & -1 & -1 & 1 & 0 & 0 \\ \cos\alpha & -\mathrm{j}\cos\alpha & 1 & -\mathrm{j} & -\mathrm{j}\mu\sin\alpha & 0 \\ \sin\alpha & -\mathrm{j}\sin\alpha & 0 & 0 & \mathrm{j}\mu\cos\alpha & \mathrm{j}\mu \end{bmatrix} \begin{bmatrix} A \\ B \\ C \\ D \\ F \\ G \end{bmatrix} = \begin{bmatrix} -\cos\alpha \\ -\sin\alpha \\ \mathrm{j} \\ 1 \\ -\mathrm{j}\cos\alpha \\ -\mathrm{j}\sin\alpha \end{bmatrix}. \tag{16}$$

in which α is the coupling angle and the non-dimensional variable $\mu = S\lambda/Ik^3$ is the only structural parameter, presented by Kil et al. [9] as a non-dimensional frequency, which can also be expressed as the wave number ratio

$$\mu = \frac{S\lambda}{Ik^3} = \left(\frac{ES}{\rho I\omega^2}\right)^{1/4} = \frac{k}{\lambda}. \tag{17}$$

This problem has an analytical solution:

$$\begin{bmatrix} A \\ B \\ C \\ D \\ F \\ G \end{bmatrix} = \begin{bmatrix} \frac{(1+j\mu^2)\sin^2\alpha}{K(\alpha,\mu)} \\ \frac{(1-\mu^2)\sin^2\alpha - j\mu(1-\cos\alpha)^2}{K(\alpha,\mu)} \\ \frac{(-1+j\mu^2)\sin^2\alpha - \mu(1-j)(1-\cos\alpha)^2}{K(\alpha,\mu)} \\ \frac{j(1-\mu^2)\sin^2\alpha + 2\mu(1+\cos\alpha)^2}{K(\alpha,\mu)} \\ \sin\alpha\,\frac{(\mu(3-j)-3-j)\cos\alpha+(1+j)(\mu+j)}{K(\alpha,\mu)} \\ \sin\alpha\,\frac{(1+j)(-\mu+j)\cos\alpha-\mu(3-j)-3-j}{K(\alpha,\mu)} \end{bmatrix}, \tag{18}$$

with

$$K(\alpha,\mu) = \mu(3 + 2\cos\alpha + 3\cos^2\alpha) + (\mu^2 + j)(1 - j)\sin^2\alpha. \tag{19}$$

2.2. Application

In this section it will be shown that the behaviour of the structure can be classified into two categories, highly sensitive to connecting angle or not. The first point is to find an indicator that could be able to determine in which category the considered structure should be classified.

A particular case is considered. The chosen beams have the same characteristics: square sections (1 cm × 1 cm), Young's modulus $E = 2.1 \times 10^{11}$ Pa, density $\rho = 7800$ kg/m^3, and the calculation is performed at frequency $f = 100$ Hz. Thus the value of the non-dimensional parameter μ is 53.5. The evolution of the amplitude of propagative waves, which are responsible for far-field structural vibration behaviour is investigated. Fig. 2 shows the amplitudes of propagative waves versus coupling angle α. According to Eq. (3), the continuous line is obtained by plotting the modulus of amplitudes of the transmitted propagative bending wave ($||D||$). One should note that this value corresponds to the choice of using unit amplitude impinging wave.

In this figure, one can define distinct zones when the coupling angle increases: if the coupling angle is equal to zero, the incident wave is fully transmitted, since the beam is an infinite one without any discontinuity. As soon as the value of α has a non-null value, the amplitude of the transmitted wave quickly decreases, and for this case, sensitivity of response to coupling angle has a large value on 0–20° range. Then, if the coupling angle is still growing, one can define a large angle range on which the sensitivity is very low. Beyond, another high-sensitivity behaviour zone can be observed, and finally the amplitude of propagative transmitted wave is null when coupling angle reaches its maximum theoretical value of 180°.

A similar analysis can be made considering bending reflected wave, and results are comparable, excepted opposite zones corresponding to total transfer or null transfer, which are reversed compared with transmitted waves analysis, as shown in Fig. 2.

Calculation also allows one to obtain the amplitudes of transmitted and reflected longitudinal waves. These curves present again high-sensitivity zones when the coupling angle is close to zero

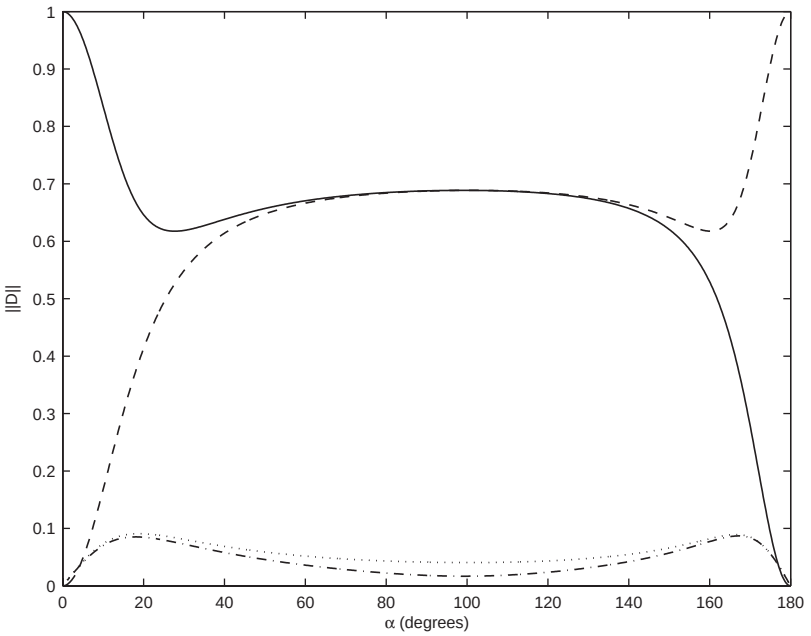

Fig. 2. Modulus of amplitudes of propagative waves versus coupling angle. –, bending transmitted wave; - -, bending reflected wave; …, longitudinal transmitted wave; –·, longitudinal reflected wave.

or 180° (see Fig. 2). However, in a vibro-acoustic process, one is mainly interested in bending movements, which are responsible for sound radiation.

Since the considered problem can be formulated using only one variable which is the wave number ratio μ, it could be interesting to obtain an expression of a critical angle versus μ, for which response sensitivity would be maximum. In order to choose the way this critical angle should be defined, the derivatives of propagating bending wave amplitudes are plotted with respect to the coupling angle α. This is done in Fig. 3.

High-sensitivity zones can be found again in this figure. The first one is centered on an angle of approximately 12°, while the second one is centered on an angle of about 170°. Unfortunately, it is not possible to define a precise value for critical angles that would be a characteristic information for high-sensitivity zones, since both transmitted and reflected waves do not reach their maximum sensitivity for the same coupling angle. A way to break this limit, is to consider a power analysis of the structure.

2.3. Power flow balance

It is possible to obtain analytical expressions for powers, but for sake of simplicity complete expressions are not detailed here. Considered power flows are defined on the basis that the incoming wave w_i is an input power of a part of the beam of which the normal vector is oriented in the $x_1 < 0$ direction, which involves sign inversions in constitutive laws (6)–(8). This sign convention is also valid for both transmitted and reflected power flows. Distinguishing between

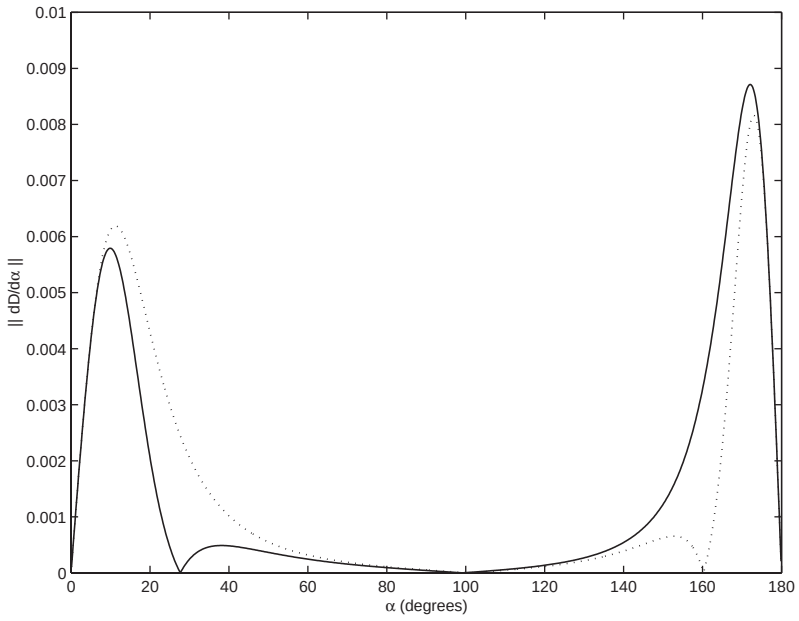

Fig. 3. Derivate of modulus of propagative bending waves with respect to coupling angle α, versus this angle. –, transmitted wave; ⋯, reflected wave.

the different transmission paths:

Power transmitted by shear force:

$$P_T(x_2) = \tfrac{1}{2}\,\mathrm{Re}(\overline{\dot{w}_t} T_t), \tag{20}$$

$$P_T(x_2) = \tfrac{1}{2} EI\omega k^3 (\|D\|^2 + \mathrm{e}^{-kx_2}\,\mathrm{Re}(\mathrm{j} C\bar{D}\mathrm{e}^{\mathrm{j}kx_2} + \bar{C}D\mathrm{e}^{-\mathrm{j}kx_2})). \tag{21}$$

Power transmitted by bending moment:

$$P_M(x_2) = \tfrac{1}{2}\,\mathrm{Re}(\overline{\dot{\Omega}_t} M_t), \tag{22}$$

$$P_M(x_2) = \tfrac{1}{2} EI\omega k^3 (\|D\|^2 - \mathrm{e}^{-kx_2}\,\mathrm{Re}(C\bar{D}\mathrm{e}^{\mathrm{j}kx_2} - \mathrm{j}\bar{C}D\mathrm{e}^{-\mathrm{j}kx_2})). \tag{23}$$

Thus the power transmitted by shear force and bending moment depend on the point of calculation, the total bending transmitted power is independent of x and remains constant all along beam 2 since:

$$P_{bending} = P_T(x_2) + P_M(x_2) = EI\omega k^3 \|D\|^2. \tag{24}$$

As far as the total transmitted power is concerned, one must first take into account the third transmission path which is due to longitudinal waves:

$$P_{longi} = \tfrac{1}{2}\,\mathrm{Re}(\overline{\dot{u}_t} N_t) = \tfrac{1}{2}\omega\lambda ES \|G\|^2. \tag{25}$$

Then, the total transmitted power does not depend on the point chosen for its evaluation:

$$P_{trans} = EI\omega k^3 \|D\|^2 + \tfrac{1}{2} ES\omega\lambda \|G\|^2. \tag{26}$$

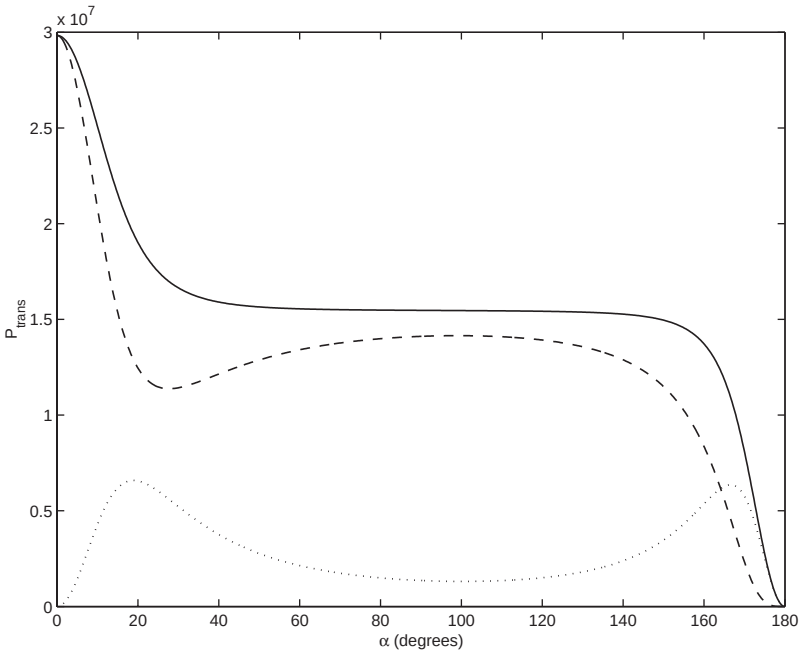

Fig. 4. Transmitted powers versus coupling angle. –, total; - -, bending; ⋯, in-plane.

Note that this power, which is plotted versus coupling angle in Fig. 4, allows one to find again which angle ranges are highly sensitive. One should note that the values of power, which are of the order of 10^7, correspond to the use of a unit impinging wave.

As far as incident power is concerned:

$$P_{inc} = \tfrac{1}{2}\,\mathrm{Re}(\overline{\dot{w}_i} T_i) + \tfrac{1}{2}\,\mathrm{Re}(\overline{\dot{\Omega}_i} M_i), \tag{27}$$

$$P_{inc} = \frac{1}{2}\,\mathrm{Re}\left(\overline{\dot{w}_i} EI \frac{\mathrm{d}^3 w_i}{\mathrm{d}x^3}\right) + \frac{1}{2}\,\mathrm{Re}\left(-\overline{\dot{\Omega}_i} EI \frac{\mathrm{d}^2 w_i}{\mathrm{d}x^2}\right), \tag{28}$$

$$P_{inc} = EI\omega k^3. \tag{29}$$

And, finally, reflected power can be written as

$$P_{refl} = \tfrac{1}{2}\,\mathrm{Re}(\overline{\dot{w}_r} T_r) + \tfrac{1}{2}\,\mathrm{Re}(\overline{\dot{\Omega}_r} M_r) + \tfrac{1}{2}\,\mathrm{Re}(\overline{\dot{u}_r} N_r), \tag{30}$$

$$P_{refl} = -EI\omega k^3 \|B\|^2 - \tfrac{1}{2} ES\omega\lambda \|F\|^2. \tag{31}$$

The three ways of reflection are illustrated in Fig. 5, in which one can find sensitive coupling angle ranges.

Thus, power flow balance applied to the considered part of the structure can be easily written since our model does not take into account any losses:

$$P_{inc} + P_{refl} = P_{trans}, \tag{32}$$

where $P_{inc} > 0$; $P_{refl} < 0$; $P_{trans} > 0$, which is in accordance with propagation direction of each considered wave.

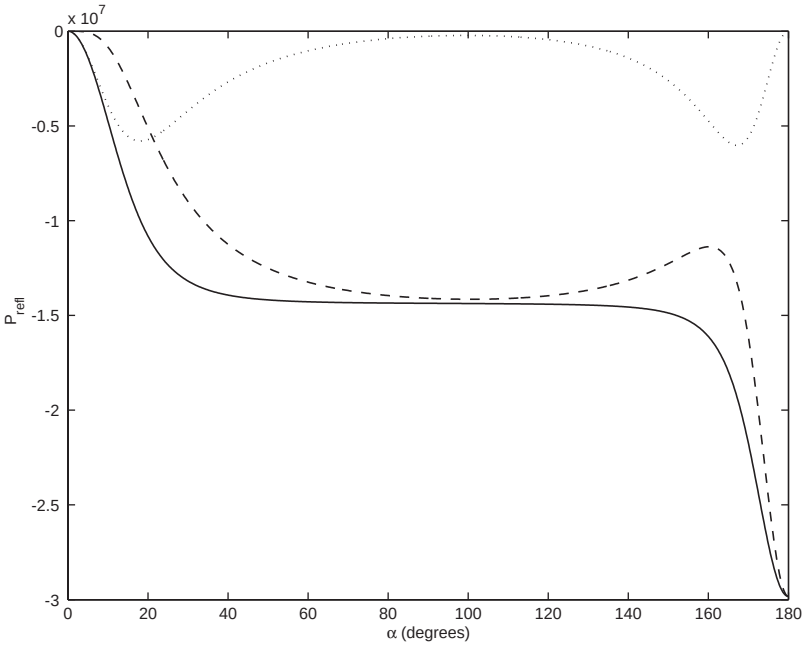

Fig. 5. Reflected powers versus coupling angle. –, total; --, bending; ⋯, in-plane.

The interest of the power analysis is that transmitted and reflected waves sensitivity to coupling angles are identical, thanks to power balance, since incoming power does not depend on the coupling angle value. In Fig. 6, the power derivative curve is presented, allowing one to define two angles for which the sensitivity is very high. The first angle has a value of 10° whereas the second one is 172°. These results are in accordance with those concerning displacements analysis, and the interest is that one can characterize the structure by two "critical" angles, around which transmitted (or reflected) power sensitivity is large. These critical angles characterize the structure sensitivity to coupling angle, which is due to rapid changes of power flow.

2.4. Critical angle values

It has been shown that the formulation uses only one variable, which is the wave number ratio. Thus it is possible to calculate critical angles versus parameter μ. Fig. 7 shows numerical results: critical angle values are plotted versus μ, which belongs to classical structure ranges.

One should note that the small critical angle does not always exist. Indeed, when $\frac{1}{3}<\mu<3$, there is only one maximum on sensitivity curve, which is above 90°. The limit case between existence and non-existence of the first angle is shown in Fig. 8.

2.5. Conclusion on coupled semi-infinite beams

Finally, it has been shown that for semi-infinite coupled beams, only one structural parameter was enough to characterize the sensitivity of the structure with respect to coupling angle. The

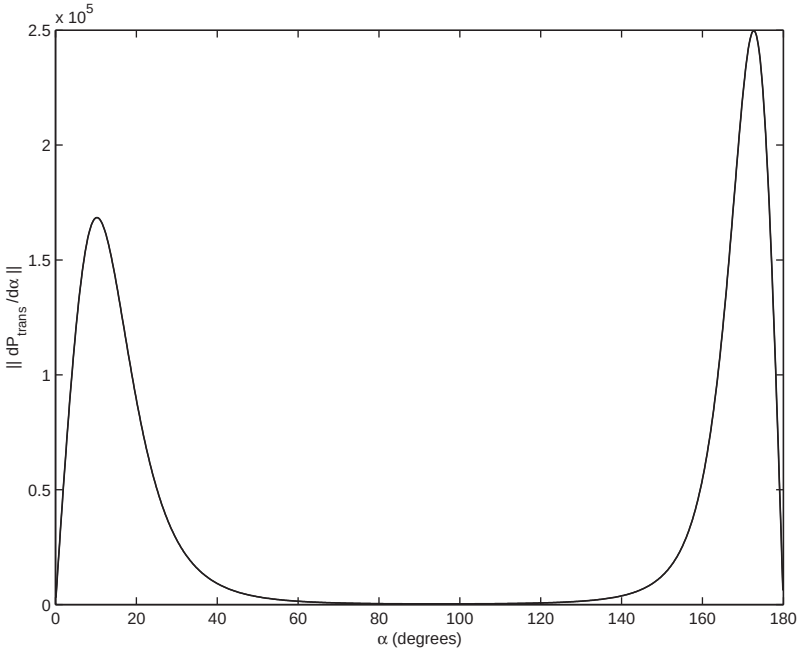

Fig. 6. Sensitivity of power versus coupling angle.

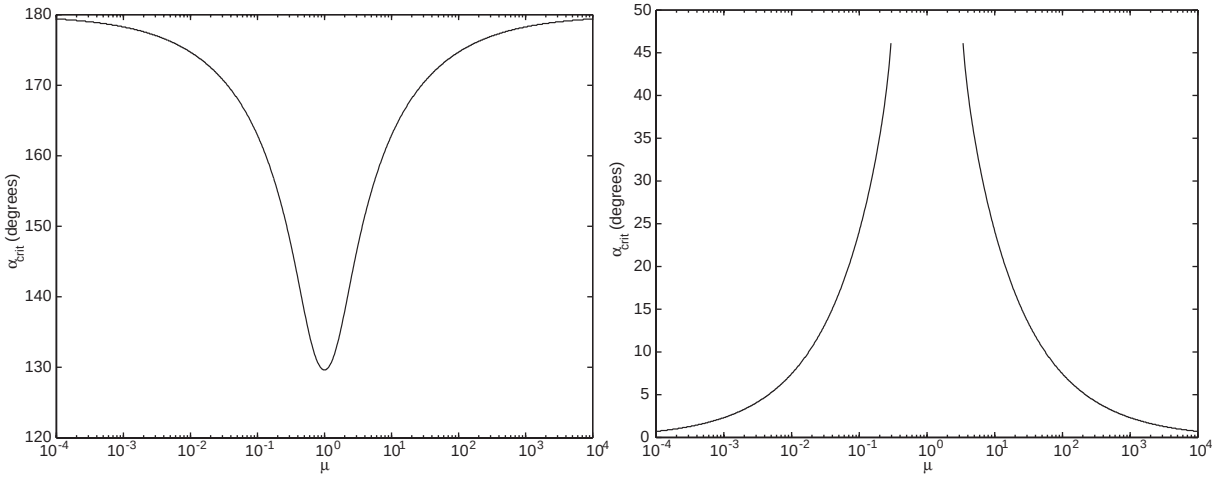

Fig. 7. Critical angles (degrees) versus wave number ratio μ.

existence of a critical angle is due to the rapid changes of power flow. The parameter used here is the wave number ratio. In most cases envisaged, two critical angles can be defined, around which the sensitivity is strong. One of these has a value lower than 45°, while the other is greater than 130°. Critical angles values have been evaluated as functions of wave number ratio.

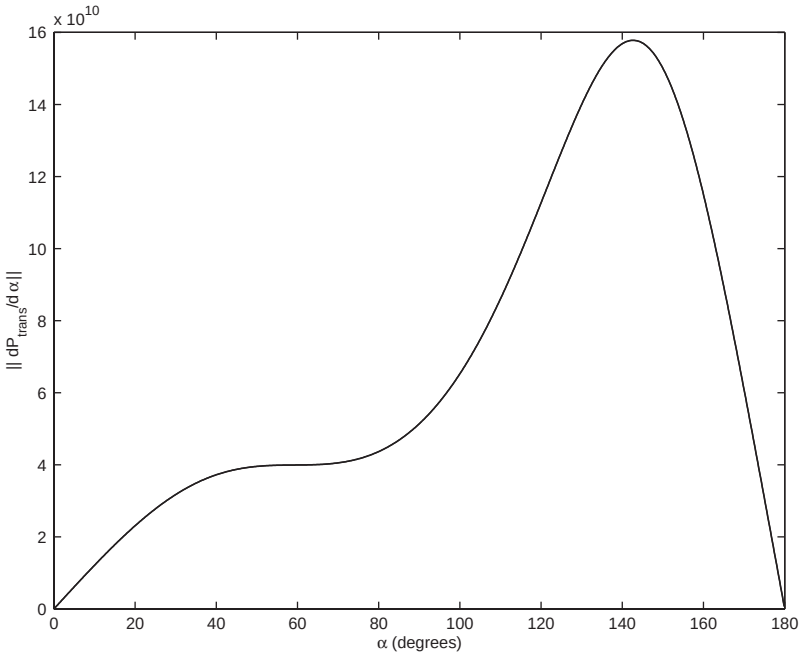

Fig. 8. Sensitivity of power versus coupling angle. Limit case.

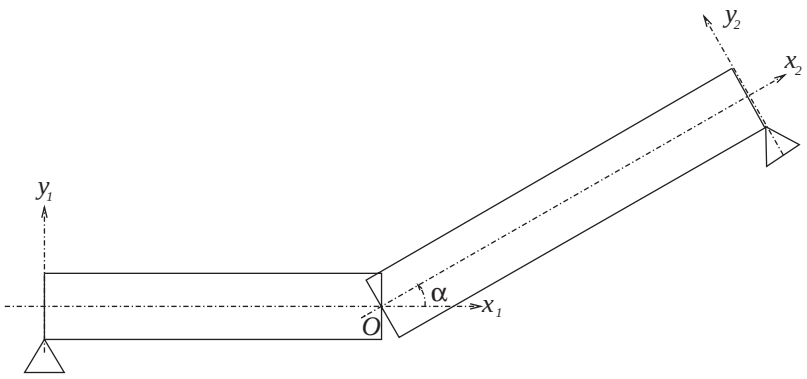

Fig. 9. Coupled finite beams.

2.6. Analysis of finite coupled beams

Previous results have been obtained using power flow analysis of semi-infinite coupled beams, so one can wonder if critical angles which have been defined in this way can be linked with results concerning finite structures.

Two finite beams, which are described in Fig. 9, are coupled with an angle α, and simply supported on both ends. Notations for this structure are detailed in Appendix E. A modal analysis of these coupled beams is presented here.

The equations of motion for beams 1 ($x_1 \in [0, L_1]$) and 2 ($x_2 \in [-L_2, 0]$) are ($i = 1$ and 2):

$$\rho_i S_i \omega^2 w_i(x_i) - E_i I_i \frac{\mathrm{d}^4 w_i(x_i)}{\mathrm{d}x_i^4} = 0,$$

$$\rho_i S_i \omega^2 u_i(x_i) + E_i S_i \frac{\mathrm{d}^2 u_i(x_i)}{\mathrm{d}x_i^2} = 0. \tag{33}$$

This is a very classical problem, its general solution can be written using this form

$$w_i(x_i) = \alpha_i \cos k_i x_i + \beta_i \sin k_i x_i + \gamma_i \operatorname{ch} k_i x_i + \delta_i \operatorname{sh} k_i x_i, \tag{34}$$

$$u_i(x_i) = \varepsilon_i \cos \lambda_i x_i + \xi_i \sin \lambda_i x_i, \tag{35}$$

in which wave numbers are

$$k_i^4 = \frac{\rho_i S_i \omega^2}{E_i I_i}, \tag{36}$$

$$\lambda_i^2 = \omega^2 \frac{\rho_i}{E_i}. \tag{37}$$

Boundary conditions at points $x_i = 0$ can be used in order to simplify the above equations by cancelling α_i, γ_i and ξ_i coefficients. Coupling conditions at points $x_1 = L_1$ and $x_2 = -L_2$ are similar to Eqs. (10)–(15), and allow one to obtain this linear system:

$$\mathbf{TX} = \mathbf{0}. \tag{38}$$

in which $\mathbf{X}^{\mathrm{T}} = [\beta_1 \ \ \delta_1 \ \ \beta_2 \ \ \delta_2 \ \ \xi_1 \ \ \xi_2]$ and

$$\mathbf{T} = \begin{bmatrix}
\sin k_1 L_1 & \operatorname{sh} k_1 L_1 & \sin k_2 L_2 \cos\alpha & \operatorname{sh} k_2 L_2 \cos\alpha & 0 & -\cos\lambda_2 L_2 \sin\alpha \\
0 & 0 & -\sin k_2 L_2 \sin\alpha & -\operatorname{sh} k_2 L_2 \sin\alpha & \cos\lambda_1 L_1 & -\cos\lambda_2 L_2 \cos\alpha \\
\cos k_1 L_1 & \operatorname{ch} k_1 L_1 & -\frac{k_2}{k_1}\cos k_2 L_2 & -\frac{k_2}{k_1}\operatorname{ch} k_2 L_2 & 0 & 0 \\
-\sin k_1 L_1 & \operatorname{sh} k_1 L_1 & -\frac{k_2^2}{k_1^2}\sin k_2 L_2 & \frac{k_2^2}{k_1^2}\operatorname{sh} k_2 L_2 & 0 & 0 \\
\cos k_1 L_1 & -\operatorname{ch} k_1 L_1 & -\frac{E_2 I_2 k_2^3}{E_1 I_1 k_1^3}\cos k_2 L_2 \cos\alpha & \frac{E_2 I_2 k_2^3}{E_1 I_1 k_1^3}\operatorname{ch} k_2 L_2 \cos\alpha & 0 & \frac{E_2 S_2 \lambda_2}{E_1 I_1 k_1^3}\sin\lambda_2 L_2 \sin\alpha \\
0 & 0 & \frac{E_2 I_2 k_2^3}{E_1 S_1 \lambda_1}\cos k_2 L_2 \sin\alpha & -\frac{E_2 I_2 k_2^3}{E_1 S_1 \lambda_1}\operatorname{ch} k_2 L_2 \sin\alpha & -\sin\lambda_1 L_1 & \frac{E_2 S_2 \lambda_2}{E_1 S_1 \lambda_1}\sin\lambda_2 L_2 \cos\alpha
\end{bmatrix}. \tag{39}$$

The eigenvalues of the structure are finally obtained with a numerical solution of the non-linear equation $\det(\mathbf{T}) = 0$.

2.7. Numerical application

The chosen characteristics are: $E_i = 2.1 \times 10^{11}$ Pa, $\rho_i = 7800$ kg m^{-3}, $L_1 = 35$ cm, $L_2 = 27$ cm. Beams rectangular section are identical (3 cm × 1 cm). Then, numerical solution of $\det(\mathbf{T}) = 0$ allows one to obtain Fig. 10, in which the 10 first eigenfrequencies of the structure are plotted versus coupling angle α. Some of these frequencies are very sensitive to coupling angle, in particular those corresponding to modes 4, 6, 8 and 10. One can note that these situations are generally local modes of one beam or correspond to in-phase vibrating beams.

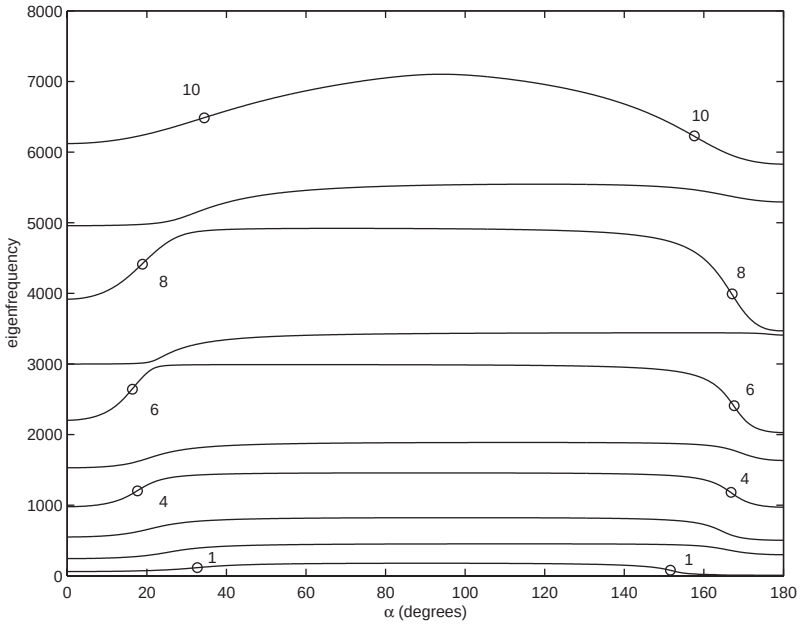

Fig. 10. Ten first eigenfrequencies (Hz) versus coupling angle (degrees). Symbols o denote inflexion points of curves.

2.8. Relationship between critical angle and eigenfrequency sensitivity

In Fig. 10, inflexion points are indicated, corresponding to angle for which sensitivity of considered eigenfrequency with respect to coupling angle reaches its maximum value. Each of these points can be used in order to define a "critical angle" associated with an eigenfrequency, allowing one to calculate the corresponding wave number ratio using Eq. (17). This set of points can be plotted in Fig. 7, which characterizes the critical angles for semi-infinite beams. This is done in Fig. 11, on which one can observe that critical angles defined using energy considerations of coupled semi-infinite beams are close to the ones defined using the sensitivity of eigenfrequencies of coupled finite beams. The only point which is not really close to the original curve is the one associated with the first mode, but as far as this particular mode is concerned, one can observe in Fig. 10 that the variation of its eigenfrequency is quite slow when coupling angle grows: in this kind of situation, the use of a so-defined critical angle has less meaning compared with a more sensitive mode, like the fourth one.

2.9. Conclusions on coupled beams

An analysis of coupled beams has been carried out in order to show that the behaviour of such a simple structure could be very sensitive to coupling angle. This phenomena has been described using semi-infinite beams, for which it has been shown that the critical coupling angle was defined using only one parameter, which is the wave number ratio. This analysis has been done considering power flows, and can be validated considering finite coupled beams, for which it has been shown that eigenfrequencies variations versus coupling angle could be linked to results obtained with semi-infinite beams.

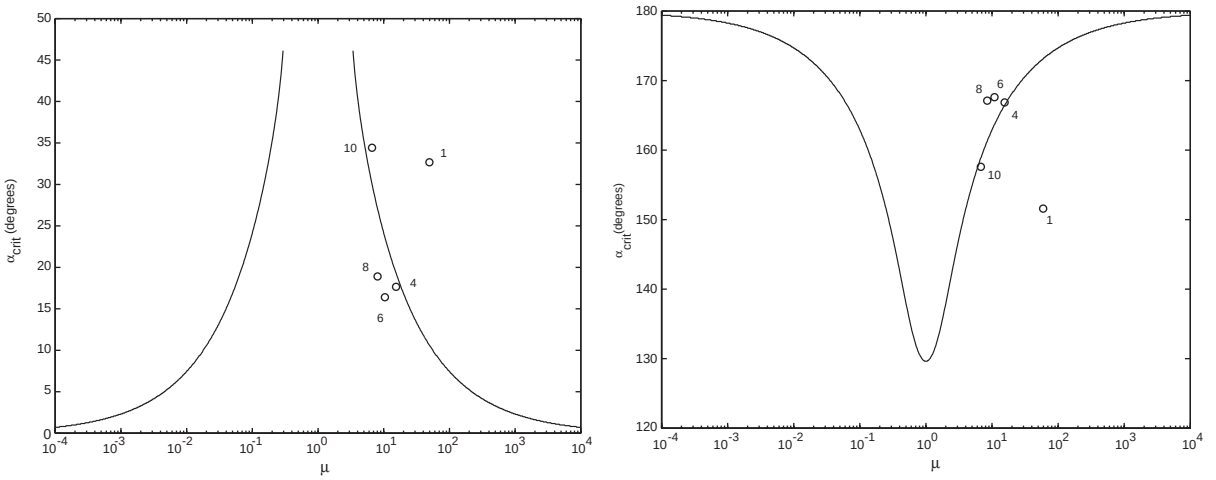

Fig. 11. Critical angle versus wave number ratio μ. -, coupled semi-infinite beams; o, values obtained for modes of finite coupled beam.

3. Coupled plates study

In this section a similar study is presented, based on semi-infinite coupled identical plates. Hypersensitivity phenomenon have been observed in coupled plates [4], that is why one can wonder if some simple rules like the ones presented above for beams exist for coupled plates.

Notations used for the forced waves decomposition are detailed in Appendix F.

3.1. Bending movement

Suppose that an incident bending wave of incidence angle θ is travelling in plate number 1, as shown in Fig. 12. This incident wave is denoted as

$$w_i = \mathrm{e}^{-\mathrm{j}k_x x - \mathrm{j}k_y y}, \tag{40}$$

in which $k_x = k\cos\theta$, $k_y = k\sin\theta$ and bending wave number k satisfies the dispersion equation:

$$k^2 = \omega\sqrt{\frac{\rho h}{D}}. \tag{41}$$

This wave is partly reflected on plate 1, while another part is transmitted on plate 2, connecting angle couples bending and in-plane vibrations because of the boundary conditions on the joint line. Taking into account spatial coincidence along a coupling line and denoting $k_e = k\sqrt{1+\cos^2\theta}$ the near-field wave number, reflected bending wave w_r and transmitted one w_t can be written as

$$\begin{aligned} w_r &= \mathrm{e}^{-\mathrm{j}k_x x}(A\mathrm{e}^{\mathrm{j}k_y y} + B\mathrm{e}^{k_e y}),\\ w_t &= \mathrm{e}^{-\mathrm{j}k_x x}(H\mathrm{e}^{-\mathrm{j}k_y y} + K\mathrm{e}^{-k_e y}). \end{aligned} \tag{42}$$

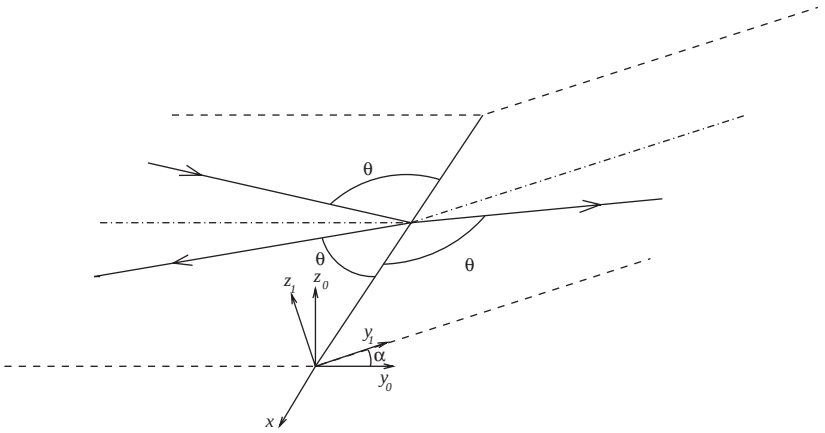

Fig. 12. Two semi-infinite coupled plates.

3.2. In-plane vibrations

Continuity conditions along a joint line introduce coupling effects between bending and in-plane vibrations. Details are given in Appendix A, and complete equations and derivations can be found in Ref. [9].

One should distinguish two types of in-plane waves, the longitudinal ones (which are parallel to the propagation direction), with a wave number λ, and the in-plane shear ones (which are perpendicular to propagation direction), corresponding to another wave number μ.

The nature of in-plane waves depends on corresponding wave number values in comparison with imposed bending one. The most frequent situation is the case numbered 3 in Appendix A, when x component of imposed bending wave number is greater than in-plane stress wave number: $k_x > \mu$.

In this situation, all existing in-plane waves are vanishing ones, corresponding to y components of wave numbers:

$$\begin{aligned} k_{ly} &= \mathrm{j}\sqrt{-\lambda^2 + k_x^2}, \\ k_{sy} &= \mathrm{j}\sqrt{-\mu^2 + k_x^2}. \end{aligned} \tag{43}$$

Reflected in-plane waves u_r, v_r and transmitted ones u_t, v_t can be expressed as follows:

$$\begin{aligned} u_r &= \mathrm{e}^{-\mathrm{j}k_x x}\left(\frac{k_x}{k} C\mathrm{e}^{-\mathrm{j}k_{ly}y} - \frac{k_{sy}}{k} P\mathrm{e}^{-\mathrm{j}k_{sy}y}\right), \\ v_r &= \mathrm{e}^{-\mathrm{j}k_x x}\left(\frac{k_{ly}}{k} C\mathrm{e}^{-\mathrm{j}k_{ly}y} + \frac{k_x}{k} P\mathrm{e}^{-\mathrm{j}k_{sy}y}\right), \end{aligned} \tag{44}$$

$$u_t = \mathrm{e}^{-\mathrm{j}k_x x}\left(\frac{k_x}{k} F \mathrm{e}^{\mathrm{j}k_{ly} y} + \frac{k_{sy}}{k} Q \mathrm{e}^{\mathrm{j}k_{sy} y}\right),$$
$$v_t = \mathrm{e}^{-\mathrm{j}k_x x}\left(-\frac{k_{ly}}{k} F \mathrm{e}^{\mathrm{j}k_{ly} y} + \frac{k_x}{k} Q \mathrm{e}^{\mathrm{j}k_{sy} y}\right). \tag{45}$$

3.3. Constitutive laws along (O, x) axis

Constitutive laws can be written along (O, x) axis to obtain expression of generalized forces, rotation and bending moment using displacement fields that will be used for continuity relation expressions:

$$F_x = \frac{Eh}{2(1+\nu)}\left(\frac{\partial u}{\partial y} + \frac{\partial v}{\partial x}\right),$$
$$F_y = \frac{Eh}{(1-\nu^2)}\left(\nu \frac{\partial u}{\partial x} + \frac{\partial v}{\partial y}\right),$$
$$F_z = -D\left(\frac{\partial^3 w}{\partial y^3} + (2-\nu)\frac{\partial^3 w}{\partial x^2 \partial y}\right), \tag{46}$$

F_x, F_y and F_z are line force densities in x, y and z directions.

$$R = \frac{\partial w}{\partial y},$$
$$M = D\left(\frac{\partial^2 w}{\partial y^2} + \nu \frac{\partial^2 w}{\partial x^2}\right). \tag{47}$$

R is the rotation angle and M is the bending moment.

3.4. Continuity relations

Eight continuity relations can be written on the junction line, in order to identify wave amplitudes. These relations are

(a) Continuity of components of displacement: $u_r = u_t$; $v_r - v_t \cos\alpha - w_t \sin\alpha = 0$; $w_i + w_r + v_t \sin\alpha - w_t \cos\alpha = 0$.
(b) Continuity of components of force: $F_x^r = F_x^t$; $F_y^r - F_y^t \cos\alpha - F_z^t \sin\alpha = 0$; $F_z^i + F_z^r + F_y^t \sin\alpha - F_z^t \cos\alpha = 0$.
(c) Continuity of rotation: $R_i + R_r - R_t = 0$ and
(d) Continuity of bending moment: $M_i + M_r - M_t = 0$.

These equations can be developed from waves in both plates and lead to the linear system of wave amplitudes that can be expressed with only four independent structural parameters: Poisson ratio ν, incidence angle of bending wave θ, coupling angle α and a non-dimensional parameter:

$$\xi = \rho \frac{h^2 \omega^2}{12E}. \tag{48}$$

Finally inversion of the system allows one to obtain the displacement field in both plates, and lastly to study the behaviour sensitivity as previously done for beams.

3.5. Numerical application

The considered structure is made of steel plates ($E = 2.1 \times 10^{11}$ Pa; $\rho = 7800$ kg/m^3; $h =$ 2 mm; $v = 0.3$), while the frequency chosen for calculation is 500 Hz and incident angle is $\theta = 40^\circ$. Thus the non-dimensional parameter is 1.2×10^{-7}. Let us observe the bending response of the structure, which is responsible for sound radiation, at several points of the structure, in order to observe near and far fields. The corresponding curves are plotted using on the one hand a point on the coupling line, since on this point evanescent and travelling waves contribute significantly to the displacement, and on the other hand another point will be used, chosen far from the junction in order that only propagative waves effects can be observed.

Fig. 13 shows that bending displacement is very sensitive to the coupling angle up to 10°. For greater angles, the bending response is not sensitive to angle variation. These observations are made for coupling angles belonging to the $0-90^\circ$ range. Beyond that, one can observe similar results to those obtained for coupled beams. These cases will be studied in Section 3.6.

As far as in-plane movements are concerned, their evolutions are plotted in Fig. 14, in which one can see that sensitive behaviour exists also for lower coupling angles. But in the present case, these waves are evanescent, and their amplitudes are decreasing fast when observation point moves away from coupling line.

To define connecting angle of maximum sensitivity, a similar remark as the one done for beams can be made: angles for which sensitivity is maximum depends on the considered wave. In order to be rid of this difficulty, transmitted and reflected powers are studied. In Fig. 15, one can observe that power is mainly transmitted by transverse velocity, whatever the coupling angle value may be, while the second transmission path is due to rotation velocity. In-plane movement does not

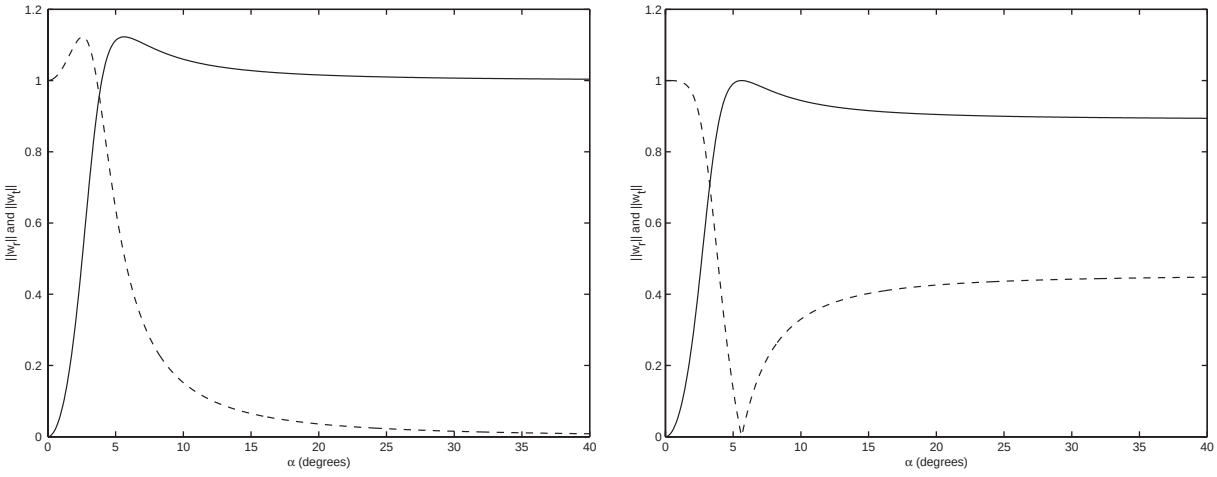

Fig. 13. Modulus of bending response versus coupling angle: (a) response on junction line, (b) response far from the junction. - -, transmitted waves; –, reflected waves.

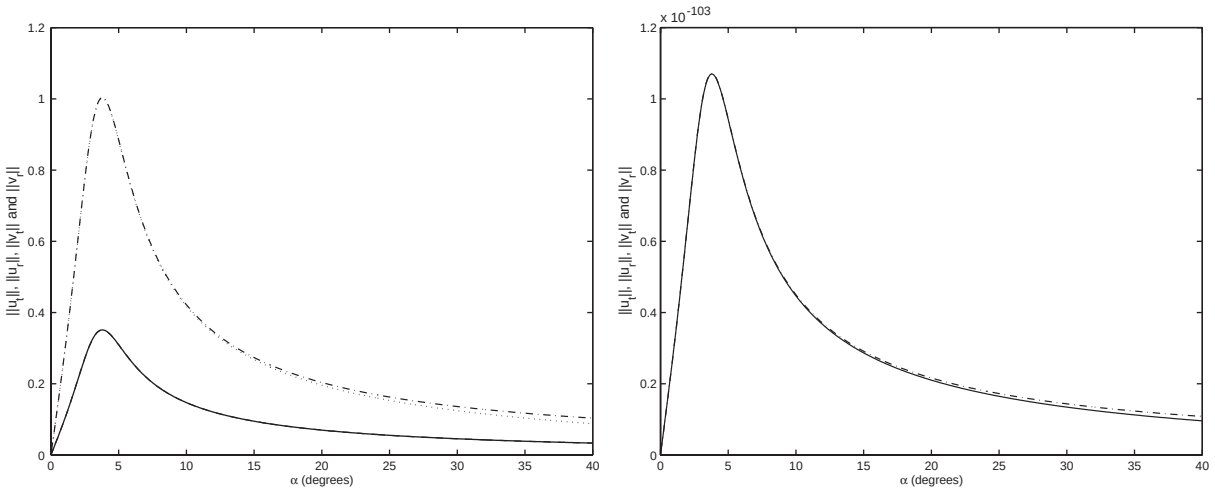

Fig. 14. Modulus of in-plane response versus coupling angle: (a) response on junction line, (b) response far from the junction. - -, transmitted u waves; –, reflected u waves; —, transmitted v waves; ··, reflected v waves.

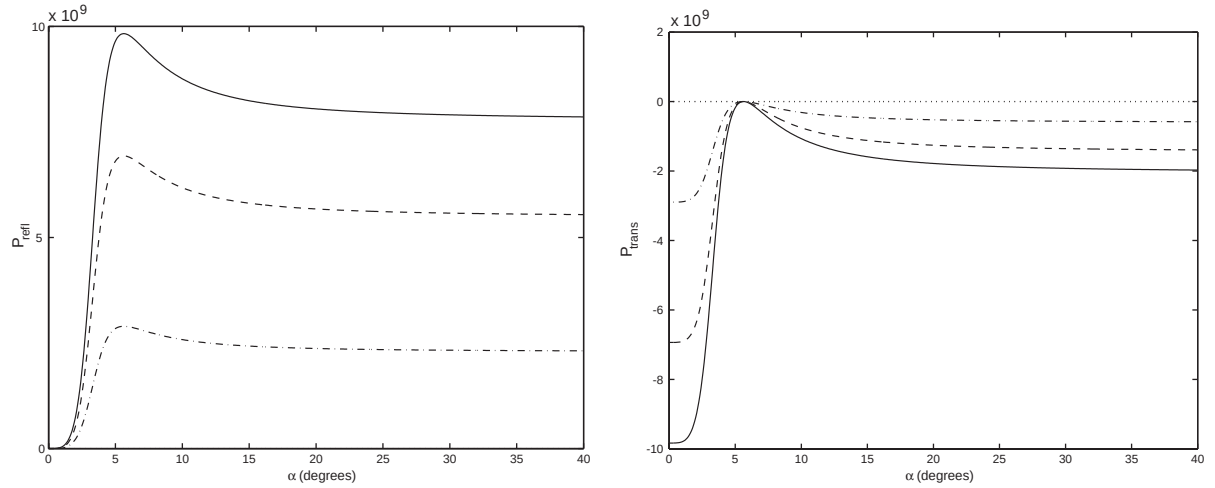

Fig. 15. Powers evolution versus coupling angle: (a) reflected powers, (b) transmitted powers. - -, bending moment power; —, shear force power; ··, in-plane power (always zero since these are close field waves); –, total power.

carry any power since associated waves are evanescent. High-sensitivity values which have been observed for small coupling angles can be found again in power evolutions, since for flat angles, reflected power is null, and grows up fast with coupling angle. In a complementary way, transmitted power is maximal for flat coupling angle, then decreases until coupling angle is 5.5°, for which power is fully reflected. Beyond, for larger angles, an equilibrium is established, and power variation is very weak when coupling angle grows.

One should be precise that the chosen parameters correspond to case number 3 ($k_x > \mu$), and for all structures belonging to that case, evolutions of displacements and powers versus coupling

angles are similar to those presented above. This behaviour is observed for most of structures: indeed, $k_x > \mu$ corresponds to

$$\frac{1-\nu}{1+\nu}\frac{3E}{4\rho\pi^2}\frac{\cos^4\theta}{h^2f^2} > 1. \tag{49}$$

If one considers steel material ($E = 2.1 \times 10^{11}$ Pa, $\rho = 7800$ kg m^{-3}, $\nu = 0.3$) or aluminum one ($E = 7.2 \times 10^{10}$ Pa, $\rho = 2700$ kg m^{-3}, $\nu = 0.34$), the previous relation can be written as

$$\frac{\cos^4\theta}{h^2f^2} > 10^{-6}. \tag{50}$$

Thus, considering the case of many incident waves, coming from each possible incident angles, one can see in Eq. (50) that the only waves that will induce propagative in-plane waves will have almost normal incidence. If one applies the above equation in the case considered ($h = 2$ mm, $f = 500$ Hz), the incidence angle value beyond which the in-plane far-field waves will appear is 88.2°. Then, if we consider an almost normal incident angle (89°), transmitted power will be mainly transported by in-plane waves. For all coupling angles with values below 88.2°, transmission will always be done by bending motion.

In order to characterize hypersensitivity, one can evaluate the critical angle when structural parameters are varied. Like for beams, the critical angle is defined by the angle α, for which the derivative of the transmitted (or reflected) power with respect to coupling angle, reaches its maximum absolute value. This calculation is performed using the three structural parameters θ, ξ and ν. The chosen ranges are $10^{-13} < \xi < 10^{-3}$, $0.2 < \nu < 0.4$ and $0° < \theta < 90°$, in order to represent most of "classical" structures and material ranges. Results are shown in Figs. 16 and 17. One can observe that in general critical angles are lower than 10°, only normal incident waves, high frequencies calculations or plates with large thicknesses bring larger critical angles. In addition, the influence of the Poisson ratio is very weak. If one tries to extrapolate these results to coupled finite plates, one can suppose that incident waves will come from many directions, and that globally there will be a range of angles for which sensitivity is important. For many situations, this will result in one particular angle that will be more sensitive than the others, and this angle is likely to be lower than 10°, which is in accordance with observed results [4].

3.6. *Behaviour of coupled plates around* $\alpha = 180°$

A similar study can be performed for angles around 180°, even if the results should be interpreted with precautions, since such structures could be impossible to build. Nevertheless, the mathematical model allows one to obtain Fig. 18, in which transmitted and reflected powers are plotted versus coupling angle. A high-sensitivity zone can be observed near 180°, which can be interpreted as the symmetric effect of the one studied in the previous section. A remark can be made about the particular value $\alpha = 180°$. In this situation, results observed for beams are no longer valid, since power is partly transmitted, because of effects along the x line, due to incidence angle θ, which is 40° in the case considered. Thus, the x component of the incident wave is not blocked by the geometry of the junction and movement is partly transmitted in plate 2.

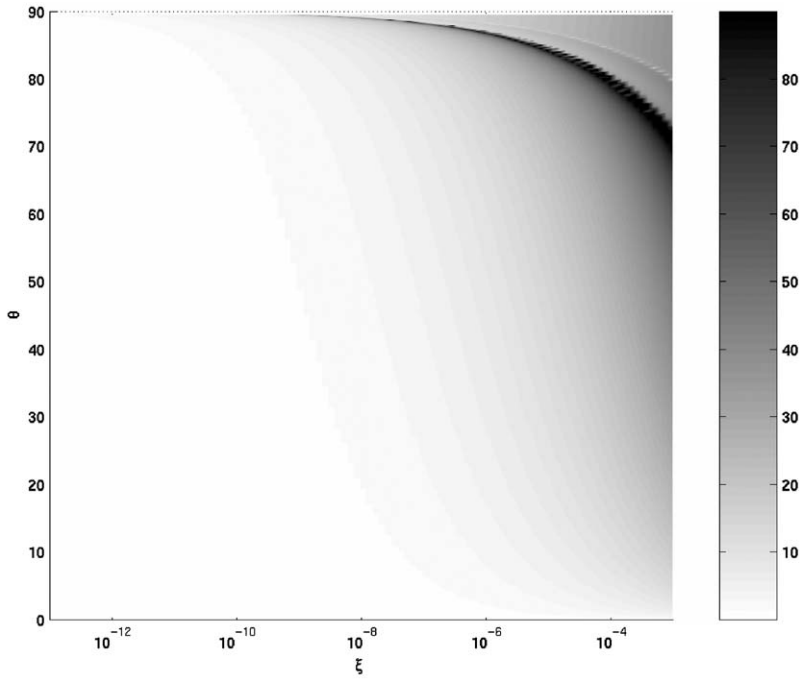

Fig. 16. Critical angle (degrees) versus incident angle θ and non-dimensional parameter ξ. $v = 0.3$.

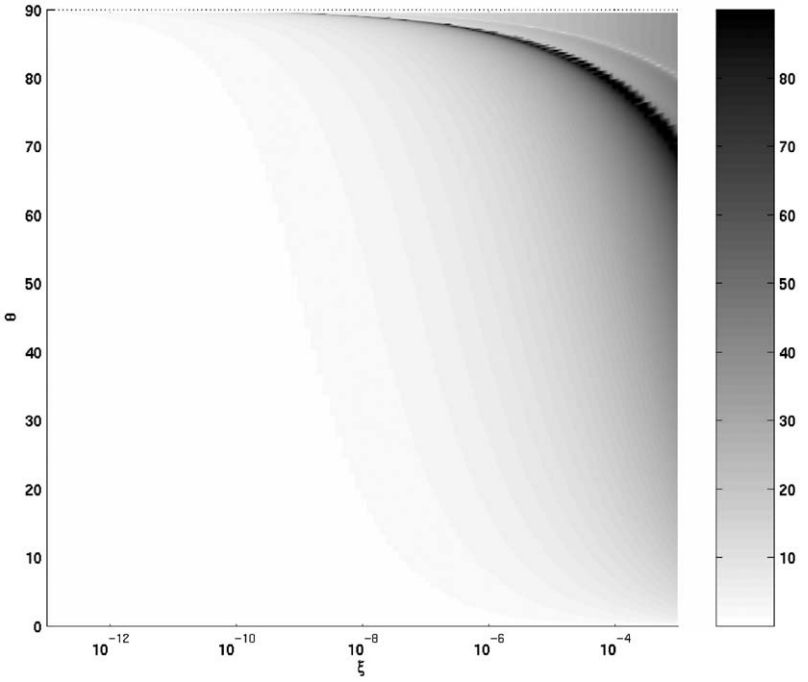

Fig. 17. Critical angle (degrees) versus incident angle θ and non-dimensional parameter ξ. $v = 0.4$.

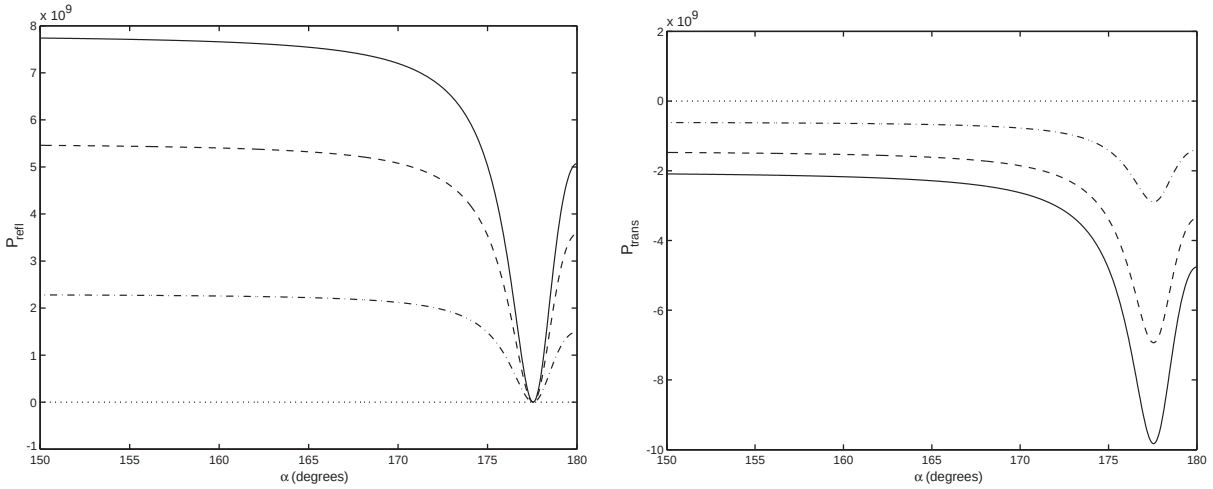

Fig. 18. Powers evolution versus coupling angle. Incident angle $\theta = 40^\circ$: (a) reflected powers, (b) transmitted powers. - -, moment; —, shear force; ··, in-plane (always zero since these are close field waves); –, total.

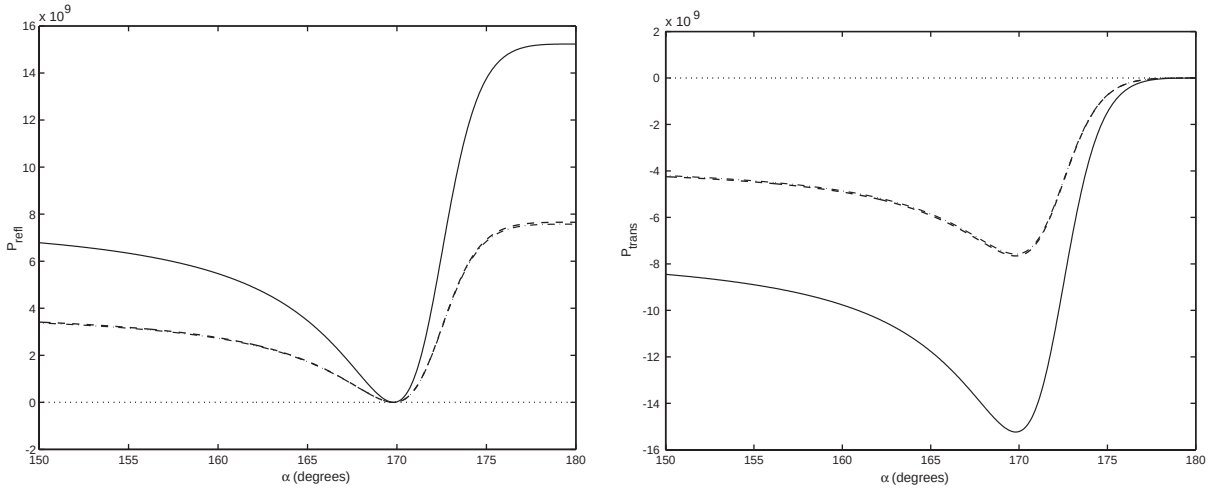

Fig. 19. Powers evolution versus coupling angle. Incident angle $\theta = 85^\circ$: (a) reflected powers, (b) transmitted powers. - -, moment; —, shear force; ··, in-plane (always zero since these are close field waves); –, total.

This figure should be compared with Fig. 19, in which the incidence angle is close to 90°. In this situation, the behaviour is close to the one observed for beams: when the coupling angle is 180°, the transmitted power is close to zero.

The high-sensitivity zone can be characterized by the angle for which the derivative of transmitted (or reflected) power with respect to connecting angle is maximum. This "critical" angle is plotted versus incident angle θ and non-dimensional parameter ξ, for $\nu = 0.3$ in Fig. 20. The gap observed around $\theta = 35^\circ$ is due to the chosen definition of critical coupling angle, and can be explained using Figs. 18 and 19. In Fig. 18, the critical angle is localized around 176°, on

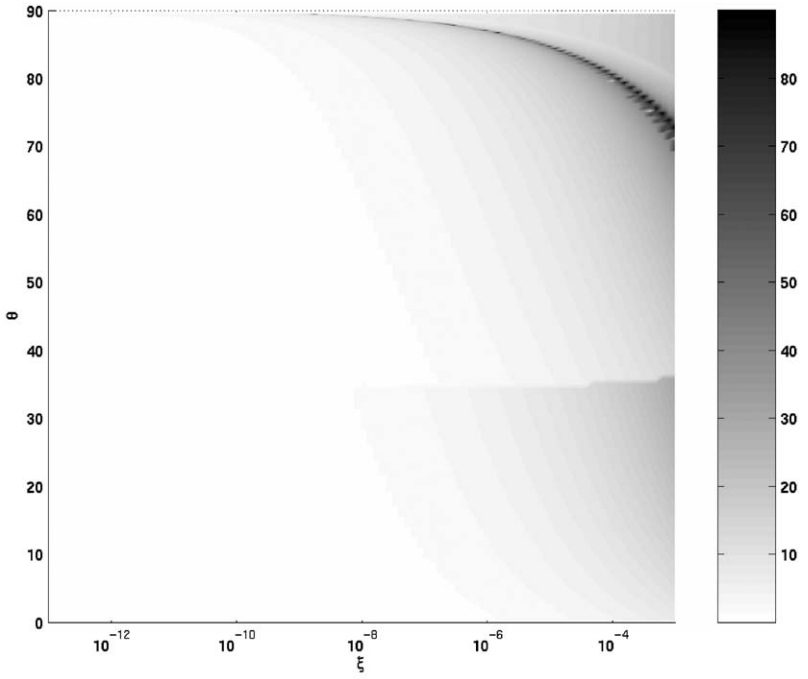

Fig. 20. Critical angle (belonging to 90–180°, plotted value is $180^\circ - \alpha_{crit}$) versus incident angle θ and non-dimensional parameter ξ. $\nu = 0.3$.

the left part of the minimum of reflected power, while as far as the picture plotted with $\theta = 85^\circ$ is concerned, critical angle is about 173°, but it is localized on the right part of the minimum of reflected power. Transition between these two situations implies the existence of the gap observed in Fig. 20.

3.7. In-plane incident waves

In order to obtain a complete description of coupled plate sensitivity phenomenon, one should wonder if the previous results are valid for in-plane incident wave. That could be important, since as far as finite coupled plates are concerned, all kinds of exciting waves can exist. The effects of an incident in-plane longitudinal wave is first studied

$$u_i = \frac{k_x}{\lambda} e^{(-jk_x x - jk_{ly} y)},$$
$$v_i = \frac{k_{ly}}{\lambda} e^{(-jk_x x - jk_{ly} y)}. \tag{51}$$

This wave is supposed to reach the coupling line with an incident angle θ:

$$k_x = \lambda \cos\theta,$$
$$k_{ly} = \lambda \sin\theta. \tag{52}$$

Complete derivation of the equations is not presented here, but the principle is exactly the same as in Sections 3.1 and 3.2. Corresponding systems are presented in Appendix C. All in-plane waves are propagative ones, but as far as bending waves are concerned, one should distinguish two cases:

- $k \geqslant k_x$ in which k is the bending wave number: $k^2 = \omega\sqrt{\rho h/D}$. In that case, propagative bending waves exist.
- $k < k_x$ then bending waves are only evanescent ones.

Note that the first case can be considered only if

$$h^2 f^2 \cos^4\theta \leqslant 9 \times 10^6, \tag{53}$$

which means that most of structures satisfy this criterion, and that reflected and transmitted bending waves are generally partly far-field ones.

Then, continuity conditions at plate junctions allow one to solve the problem, and to find the transmitted and reflected power expressions associated with incident in-plane longitudinal wave, like the one shown in Fig. 21. The main transmission path is in-plane waves. One can observe that sensitive coupling angles exist, even if sensitivity values are lower than in the previous part.

Determination of the critical angle corresponding to maximum sensitivity allows one to plot Fig. 22. One can observe that the incident angle has a very low influence on the critical angle value, except for low-angled waves, for which critical angle is lower than $10-20^\circ$ (as far as "classical" structures are concerned), which is in accordance with results concerning incident bending wave (Section 3.5).

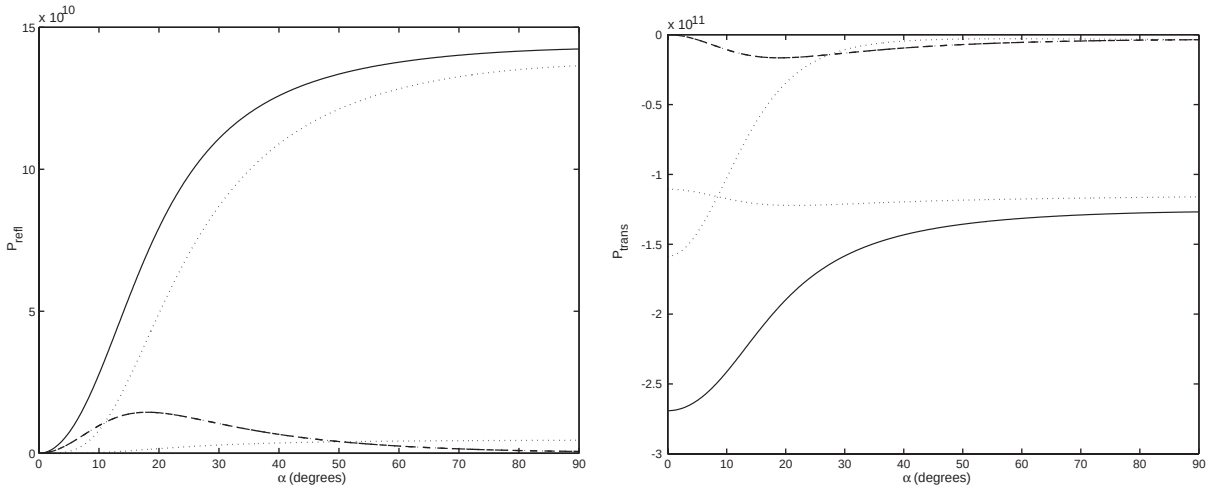

Fig. 21. Powers evolution versus coupling angle: (a) reflected powers, (b) transmitted powers. - -, moment; –·, shear force; ··, in-plane; –, total.

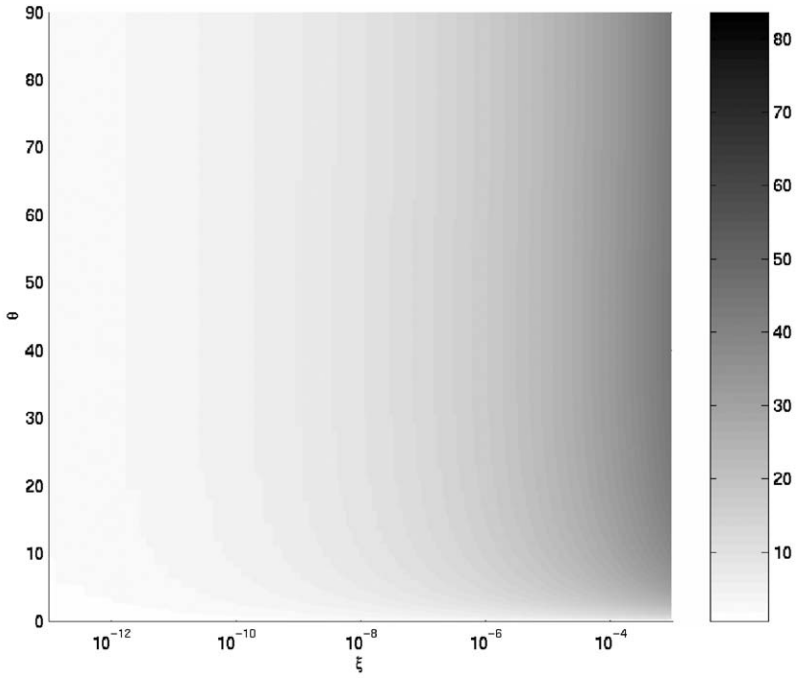

Fig. 22. Critical angle (degrees) for incident in-plane longitudinal wave versus incident angle θ and non-dimensional parameter ξ. $\nu = 0.3$.

A similar analysis can be performed to obtain Fig. 23, which shows the corresponding results based on incident in-plane shear wave, details in Appendix D

$$u_i = -\frac{k_{sy}}{\mu} e^{(-jk_x x - jk_{sy} y)},$$
$$v_i = \frac{k_x}{\mu} e^{(-jk_x x - jk_{sy} y)}, \tag{54}$$

with

$$k_x = \mu \cos\theta,$$
$$k_{sy} = \mu \sin\theta. \tag{55}$$

One can observe that the results are close to those noted above, except for very low incident angles. In those cases, there is no maximum in the sensitivity curve. This phenomenon is comparable to the one observed for coupled beams (Fig. 8).

3.8. Conclusion on semi-infinite coupled plates and extension to finite coupled plates

As far as results linked to the coupling of semi-infinite plates are concerned, there is no configuration guaranteeing that the structure not to be hypersensitive for a given excitation. Nevertheless, the general tendency is that structures with coupling angles close to zero or 180° are most likely to be hypersensitive, since a lot of configurations for which the critical angle belongs to

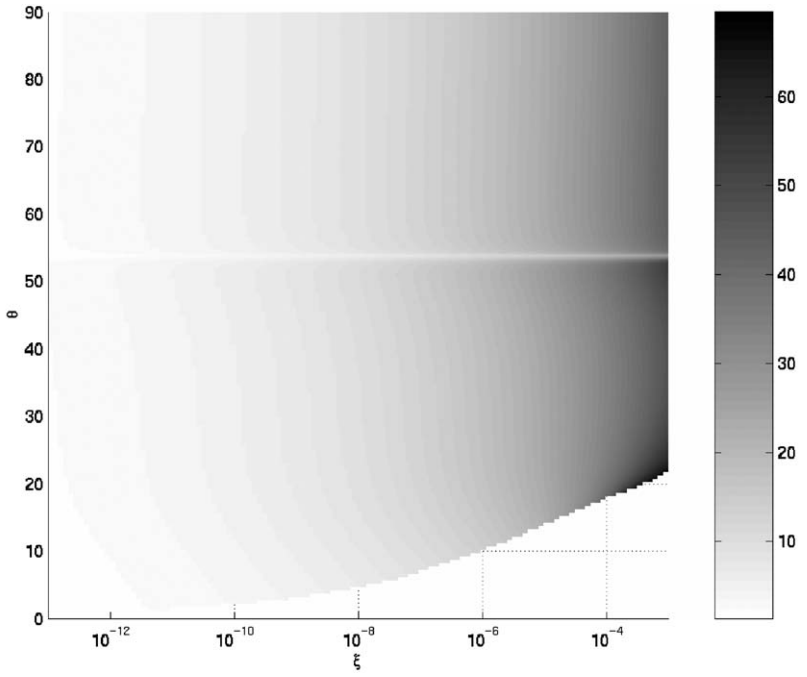

Fig. 23. Critical angle (degrees) for incident in-plane shear wave versus incident angle θ and non-dimensional parameter ξ. $\nu = 0.3$.

these ranges exist. In a general case, the three described kinds of waves can exist simultaneously, but since most of the time bending waves have generally more power than in-plane ones, the behaviour of the structure will be close to the first described one (incident bending wave).

The interesting point is that most of the critical angles are lower than 10°, and it means that for finite structures, on which incident waves are coming from all directions, there should exist a mean angle for which the structure is very sensitive to coupling angle. This mean angle depends on structure characteristics, but it is possible to affirm that in many cases it will be on the $0-10°$ range. Of course this result is a general trend and particular values of structural parameters or excitation could imply that critical angle is greater than 10°.

This can be verified using results obtained by Rébillard and Guyader [5], concerning the analysis of two finite plates, which are coupled with an angle ϕ. Dimensions of the structure are given in Fig. 24. A sensitivity indicator is defined using the transfer mobility between two points (A and B). The mobility $Y(A, B, \phi)$ is the ratio of normal velocity at point B to normal force at point A. Its variation is denoted $\delta Y(A, B, \delta\phi)$ when the coupling angle varies. The sensitivity indicator $\alpha(\phi, \delta\phi)$ is then defined as

$$\alpha(\phi, \delta\phi) = \left| \frac{\delta Y(A, B, \delta\phi)}{Y(A, B, \phi)} \right|. \tag{56}$$

Fig. 25, reproduced from Ref. [5], represents variation of α at 500 Hz when the value of $\delta\phi$ is one degree. In this case, maximum sensitivity is obtained for a coupling value of 7.5°.

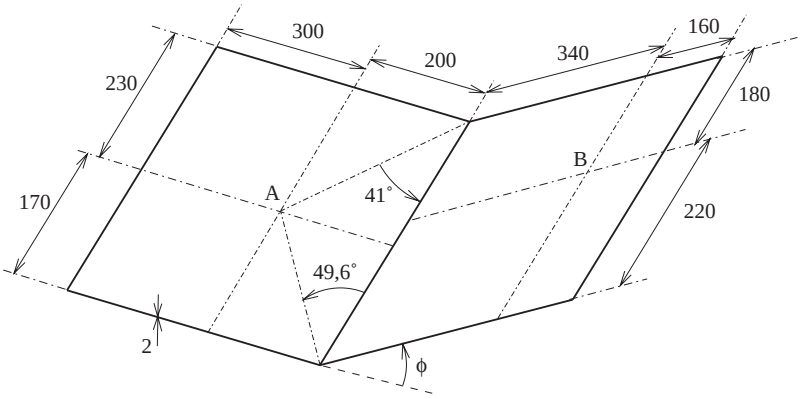

Fig. 24. Size (mm) of the coupled finite plates.

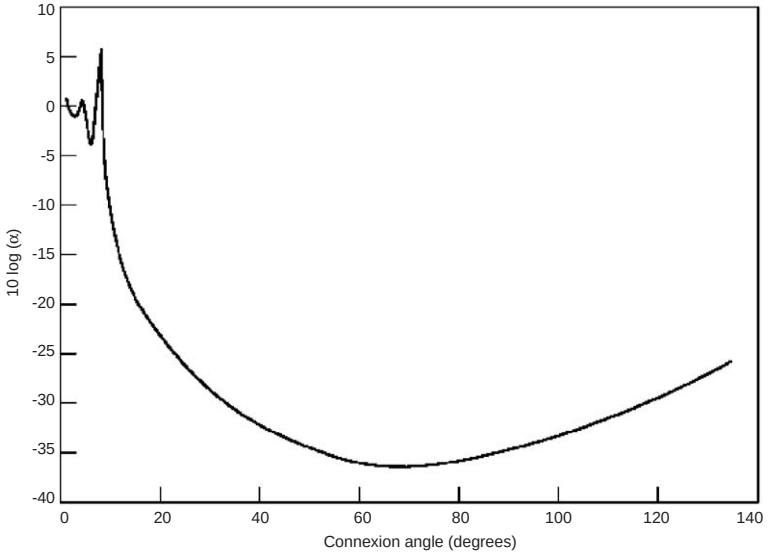

Fig. 25. Sensitivity of transfer mobility, after Ref. [5].

If one tries to compare this result with the one obtained for semi-infinite plates, one should consider the non-dimensional parameter 48, whose value in the considered case is $\xi = 1.23 \times 10^{-7}$. Fig. 26 represents a cut of Fig. 16 for such a value of ξ: it is not easy to infer from it a particular value for critical angle, since it depends on incident angle.

A simplified approach can be performed assuming that there is a direct combination of waves coming directly from point A to the coupling line, resulting in a global critical angle which is the mean of critical angles taken into account:

$$\alpha_{crit\ \ mean} = \frac{1}{\Delta\theta} \int_{\Delta\theta} \alpha_{crit}(\theta)\, \mathrm{d}\theta. \tag{57}$$

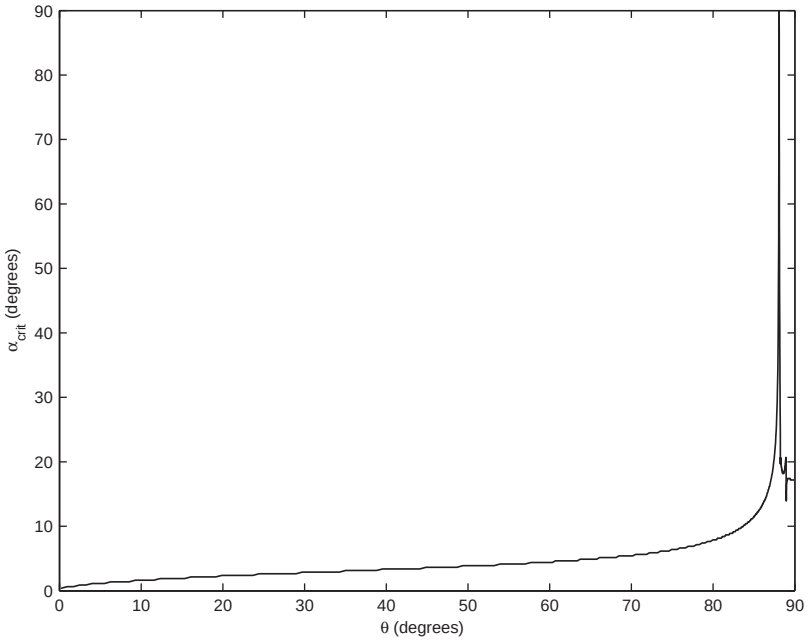

Fig. 26. Cut of Fig. 16, for $\xi = 1.23 \times 10^{-7}$: critical coupling angle versus incidence angle.

In the considered case:

$$\alpha_{crit\ \ mean} = \frac{1}{(41 + 49.6)}\left(\int_{41}^{90} \alpha_{crit}(\theta)\, \mathrm{d}\theta + \int_{49.6}^{90} \alpha_{crit}(\theta)\, \mathrm{d}\theta \right). \tag{58}$$

Indeed, the estimated critical angle for the plate considered has a value of 6.9°, which is close to the real one (7.5°). This allows one to justify the previous analysis performed on semi infinite plates.

4. Conclusions

For both structures considered (semi-infinite coupled beams and plates), a critical angle can be defined, for which the sensitivity of the transmitted (and reflected) power with respect to coupling angle is maximum. Its existence is related to rapid changes in the transmission paths, which are clearly identified by a power flow analysis. The value of this angle depends on the characteristics of both structure and excitation, but is often smaller than 10°, or close to 180°. As far as the case of beams is concerned, the wave number ratio is sufficient to know the critical angle value, where as three parameters are necessary in the case of coupled semi-infinite plates. These results can be used in order to understand the behaviour of finite structures, in which various kinds of waves exist, with many incidences, and the above results indicate that it often results in the existence of a critical angle whose value is lower than 10°.

Appendix A. In-plane vibrations

Continuity conditions along joint line introduce coupling effects between bending and in-plane vibrations. In-plane equations have been developed in Ref. [9], corresponding to the governing equations:

$$\frac{\partial^2 u}{\partial x^2}+\frac{1-\nu}{2}\frac{\partial^2 u}{\partial y^2}+\frac{1+\nu}{2}\frac{\partial^2 v}{\partial x\partial y}=-\frac{(1-\nu^2)}{E}\rho\omega^2 u, \tag{A.1}$$

$$\frac{\partial^2 v}{\partial x^2}+\frac{1-\nu}{2}\frac{\partial^2 v}{\partial y^2}+\frac{1+\nu}{2}\frac{\partial^2 u}{\partial x\partial y}=-\frac{(1-\nu^2)}{E}\rho\omega^2 v. \tag{A.2}$$

The general solution, using variable separation, can written in the following terms:

$$u=u_l+u_s,$$

$$v=v_l+v_s,$$

where one can distinguish two types of in-plane waves, the longitudinal ones (which are parallel to propagation direction)

$$u_l=k_{lx}(A_l e^{(-jk_{lx}x-jk_{ly}y)}-B_l e^{(jk_{lx}x-jk_{ly}y)}+C_l e^{(-jk_{lx}x+jk_{ly}y)}-D_l e^{(jk_{lx}x+jk_{ly}y)}),$$

$$v_l=k_{ly}(A_l e^{(-jk_{lx}x-jk_{ly}y)}+B_l e^{(jk_{lx}x-jk_{ly}y)}-C_l e^{(-jk_{lx}x+jk_{ly}y)}-D_l e^{(jk_{lx}x+jk_{ly}y)}),$$

with $k_{lx}^2+k_{ly}^2=\lambda^2=\rho\omega^2(1-\nu^2)/E$ and the in-plane shear ones (which are perpendicular to propagation direction):

$$u_s=k_{sy}(-A_s e^{(-jk_{sx}x-jk_{sy}y)}-B_s e^{(jk_{sx}x-jk_{sy}y)}+C_s e^{(-jk_{sx}x+jk_{sy}y)}+D_s e^{(jk_{sx}x+jk_{sy}y)}),$$

$$v_s=k_{sx}(A_s e^{(-jk_{sx}x-jk_{sy}y)}-B_s e^{(jk_{sx}x-jk_{sy}y)}+C_s e^{(-jk_{sx}x+jk_{sy}y)}-D_s e^{(jk_{sx}x+jk_{sy}y)}),$$

in which $k_{sx}^2+k_{sy}^2=\mu^2=2\rho\omega^2(1+\nu)/E$.

These expressions can be simplified by taking into account the fact that the plates considered plates semi-infinite, and that displacement fields should be spatially coincident along the x-axis with bending fields:

$$k_{lx}=k_x \quad \text{and} \quad k_{sx}=k_x.$$

Then, one should distinguish three cases:

Case 1: *Longitudinal wave number value is greater than x component of imposed bending wave number*, $\lambda \geqslant k_x$. Suppose that the materials considered are such that the Poisson ratio ν is lower than 0.5, thus the in-plane stress μ wave number is always greater than the longitudinal wave number λ, and for the case considered, it leads to $\mu > k_x$ since $\mu = 2(1-\nu)\lambda$.

Then, the y components of in-plane wave number values are fixed and are real and positive.

$$k_{ly}=\sqrt{\lambda^2-k_x^2},$$

$$k_{sy}=\sqrt{\mu^2-k_x^2}.$$

Corresponding waves are propagative ones, and taking into account spatial coincidence, reflected in-plane waves can be expressed as

$$u_r = \mathrm{e}^{-\mathrm{j}k_x x}\left(\frac{k_x}{k} C\mathrm{e}^{\mathrm{j}k_{ly}y} + \frac{k_{sy}}{k} P\mathrm{e}^{\mathrm{j}k_{sy}y}\right),$$

$$v_r = \mathrm{e}^{-\mathrm{j}k_x x}\left(-\frac{k_{ly}}{k} C\mathrm{e}^{\mathrm{j}k_{ly}y} + \frac{k_x}{k} P\mathrm{e}^{\mathrm{j}k_{sy}y}\right).$$

And as far as transmitted in-plane waves are concerned:

$$u_t = \mathrm{e}^{-\mathrm{j}k_x x}\left(\frac{k_x}{k} F\mathrm{e}^{-\mathrm{j}k_{ly}y} - \frac{k_{sy}}{k} Q\mathrm{e}^{-\mathrm{j}k_{sy}y}\right),$$

$$v_t = \mathrm{e}^{-\mathrm{j}k_x x}\left(\frac{k_{ly}}{k} F\mathrm{e}^{-\mathrm{j}k_{ly}y} + \frac{k_x}{k} Q\mathrm{e}^{-\mathrm{j}k_{sy}y}\right).$$

Case 2: *x Component of imposed bending wave number is greater than longitudinal wave number and smaller than in-plane stress wave number*, $\mu \geqslant k_x > \lambda$. This implies that longitudinal wave is a close-field one, while in-plane stress wave is a propagative one:

$$k_{ly} = \mathrm{j}\sqrt{-\lambda^2 + k_x^2},$$

$$k_{sy} = \sqrt{\mu^2 - k_x^2}.$$

Reflected waves can be expressed like this:

$$u_r = \mathrm{e}^{-\mathrm{j}k_x x}\left(\frac{k_x}{k} C\mathrm{e}^{-\mathrm{j}k_{ly}y} + \frac{k_{sy}}{k} P\mathrm{e}^{\mathrm{j}k_{sy}y}\right),$$

$$v_r = \mathrm{e}^{-\mathrm{j}k_x x}\left(\frac{k_{ly}}{k} C\mathrm{e}^{-\mathrm{j}k_{ly}y} + \frac{k_x}{k} P\mathrm{e}^{\mathrm{j}k_{sy}y}\right),$$

and as far as transmitted in-plane waves are concerned:

$$u_t = \mathrm{e}^{-\mathrm{j}k_x x}\left(\frac{k_x}{k} F\mathrm{e}^{\mathrm{j}k_{ly}y} - \frac{k_{sy}}{k} Q\mathrm{e}^{-\mathrm{j}k_{sy}y}\right),$$

$$v_t = \mathrm{e}^{-\mathrm{j}k_x x}\left(-\frac{k_{ly}}{k} F\mathrm{e}^{\mathrm{j}k_{ly}y} + \frac{k_x}{k} Q\mathrm{e}^{-\mathrm{j}k_{sy}y}\right).$$

Case 3: *x Component of imposed bending wave number is greater than in-plane stress wave number*, $k_x > \mu$. All existing in-plane waves are close-field ones.

$$k_{ly} = \mathrm{j}\sqrt{-\lambda^2 + k_x^2},$$

$$k_{sy} = \mathrm{j}\sqrt{-\mu^2 + k_x^2}.$$

Reflected waves can be expressed like this:

$$u_r = \mathrm{e}^{-\mathrm{j}k_x x}\left(\frac{k_x}{k} C\mathrm{e}^{-\mathrm{j}k_{ly}y} - \frac{k_{sy}}{k} P\mathrm{e}^{-\mathrm{j}k_{syy}y}\right),$$

$$v_r = \mathrm{e}^{-\mathrm{j}k_x x}\left(\frac{k_{ly}}{k} C\mathrm{e}^{-\mathrm{j}k_{ly}y} + \frac{k_x}{k} P\mathrm{e}^{-\mathrm{j}k_{syy}y}\right),$$

and as far as transmitted in-plane waves are concerned:

$$u_t = \mathrm{e}^{-\mathrm{j}k_x x}\left(\frac{k_x}{k} F\mathrm{e}^{\,\mathrm{j}k_{ly}y} + \frac{k_{sy}}{k} Q\mathrm{e}^{\,\mathrm{j}k_{syy}y}\right),$$

$$v_t = \mathrm{e}^{-\mathrm{j}k_x x}\left(-\frac{k_{ly}}{k} F\mathrm{e}^{\,\mathrm{j}k_{ly}y} + \frac{k_x}{k} Q\mathrm{e}^{\,\mathrm{j}k_{syy}y}\right).$$

Appendix B. Linear system for incident bending wave

In this appendix linear systems according to the three cases considered are presented.

- Case 1: $\mu > \lambda \geqslant k_x$.
- Case 2: $\mu \geqslant k_x > \lambda$.
- Case 3: $k_x > \mu > \lambda$.

A linear system is denoted $\mathbf{T}.\mathbf{X} = \mathbf{b}$, in which $\mathbf{X}^t = [A\ B\ C\ F\ H\ K\ P\ Q]$, corresponding to waves amplitudes defined in Sections 3.1 and 3.2. $\mathbf{T}$ is an (8×8) matrix, its expression depends on the case considered:

$$\mathbf{T} = \begin{bmatrix} \mathbf{T}_{11} & \mathbf{T}_{12} \\ \mathbf{T}_{21} & \mathbf{T}_{22} \end{bmatrix}.$$

Case 1:

$$\mathbf{T}_{11} = \begin{bmatrix} 0 & 0 & \frac{k_x}{k} & -\frac{k_x}{k} \\ 0 & 0 & \frac{k_{ly}}{k} & \frac{k_{ly}}{k}\cos\alpha \\ 1 & 1 & 0 & \frac{k_{ly}}{k}\sin\alpha \\ 0 & 0 & 2\frac{k_x k_{ly}}{k^2} & 2\frac{k_x k_{ly}}{k^2} \end{bmatrix},$$

$$\mathbf{T}_{12} = \begin{bmatrix} 0 & 0 & \frac{k_{sy}}{k} & \frac{k_{sy}}{k} \\ \sin\alpha & \sin\alpha & -\frac{k_x}{k} & \frac{k_x}{k}\cos\alpha \\ -\cos\alpha & -\cos\alpha & 0 & \frac{k_x}{k}\sin\alpha \\ 0 & 0 & \frac{k_{sy}^2 - k_x^2}{k^2} & \frac{(k_x^2 - k_{sy}^2)}{k^2} \end{bmatrix},$$

$$\mathbf{T}_{21} = \begin{bmatrix} 0 & 0 & \mathrm{j}\frac{(k_{ly}^2+\nu k_x^2)}{k^2} & -\mathrm{j}\frac{(k_{ly}^2+\nu k_x^2)}{k^2}\cos\alpha \\ \mathrm{j}\frac{D(-1+\nu^2)k_y(k_y^2+(2-\nu)k_x^2)}{Ehk} & \frac{D(-1+\nu^2)k_e(k_e^2+(2-\nu)k_x^2)}{Ehk} & 0 & \mathrm{j}\frac{(k_{ly}^2+\nu k_x^2)}{k^2}\sin\alpha \\ \mathrm{j}\frac{k_y}{k} & \frac{k_e}{k} & 0 & 0 \\ \frac{(k_y^2+\nu k_x^2)}{k^2} & \frac{(-k_e^2+\nu k_x^2)}{k^2} & 0 & 0 \end{bmatrix},$$

$$\mathbf{T}_{22} = \begin{bmatrix} \mathrm{j}\frac{D(-1+\nu^2)k_y(k_y^2+(2-\nu)k_x^2)}{Ehk}\sin\alpha & \frac{D(-1+\nu^2)k_e(-k_e^2+(2-\nu)k_x^2)}{Ehk}\sin\alpha & \mathrm{j}\frac{k_xk_{sy}(\nu-1)}{k^2} & \mathrm{j}\frac{k_xk_{sy}(\nu-1)}{k^2}\cos\alpha \\ \mathrm{j}\frac{D(-1+\nu^2)k_y(k_y^2+(2-\nu)k_x^2)}{Ehk}\cos\alpha & \frac{D(-1+\nu^2)k_e(-k_e^2+(2-\nu)k_x^2)}{Ehk}\cos\alpha & 0 & \mathrm{j}\frac{k_xk_{sy}(\nu-1)}{k^2}\sin\alpha \\ 0 & \mathrm{j}\frac{k_y}{k} & \frac{k_e}{k} & 0 \\ 0 & \frac{-k_y^2-\nu k_x^2}{k^2} & \frac{k_e^2-\nu k_x^2}{k^2} & 0 \end{bmatrix}.$$

Case 2:

$$\mathbf{T}_{11} = \begin{bmatrix} 0 & 0 & \frac{k_x}{k} & -\frac{k_x}{k} \\ 0 & 0 & -\frac{k_{ly}}{k} & -\frac{k_{ly}}{k}\cos\alpha \\ 1 & 1 & 0 & -\frac{k_{ly}}{k}\sin\alpha \\ 0 & 0 & -2\frac{k_xk_{ly}}{k^2} & -2\frac{k_xk_{ly}}{k^2} \end{bmatrix},$$

$$\mathbf{T}_{12} = \begin{bmatrix} 0 & 0 & \frac{k_{sy}}{k} & \frac{k_{sy}}{k} \\ \sin\alpha & \sin\alpha & -\frac{k_x}{k} & \frac{k_x}{k}\cos\alpha \\ -\cos\alpha & -\cos\alpha & 0 & \frac{k_x}{k}\sin\alpha \\ 0 & 0 & \frac{(k_{sy}^2-k_x^2)}{k^2} & \frac{(k_x^2-k_{sy}^2)}{k^2} \end{bmatrix},$$

$$\mathbf{T}_{21} = \begin{bmatrix} 0 & 0 & \mathrm{j}\frac{k_{ly}^2+\nu k_x^2}{k^2} & -\mathrm{j}\frac{k_{ly}^2+\nu k_x^2}{k^2}\cos\alpha \\ \mathrm{j}\frac{D(-1+\nu^2)k_y(k_y^2+(2-\nu)k_x^2)}{Ehk} & \frac{D(-1+\nu^2)k_e(k_e^2+(2-\nu)k_x^2)}{Ehk} & 0 & \mathrm{j}\frac{k_{ly}^2+\nu k_x^2}{k^2}\sin\alpha \\ \mathrm{j}\frac{k_y}{k} & \frac{k_e}{k} & 0 & 0 \\ \frac{k_y^2+\nu k_x^2}{k^2} & \frac{-k_e^2+\nu k_x^2}{k^2} & 0 & 0 \end{bmatrix},$$

$$\mathbf{T}_{22} = \begin{bmatrix} \mathrm{j}\frac{D(-1+\nu^2)k_y(k_y^2+(2-\nu)k_x^2)}{Ehk}\sin\alpha & \frac{D(-1+\nu^2)k_e(-k_e^2+(2-\nu)k_x^2)}{Ehk}\sin\alpha & \mathrm{j}\frac{k_xk_{sy}(\nu-1)}{k^2} & \mathrm{j}\frac{k_xk_{sy}(\nu-1)}{k^2}\cos\alpha \\ \mathrm{j}\frac{D(-1+\nu^2)k_y(k_y^2+(2-\nu)k_x^2)}{Ehk}\cos\alpha & \frac{D(-1+\nu^2)k_e(-k_e^2+(2-\nu)k_x^2)}{Ehk}\cos\alpha & 0 & \mathrm{j}\frac{k_xk_{sy}(\nu-1)}{k^2}\sin\alpha \\ 0 & \mathrm{j}\frac{k_y}{k} & \frac{k_e}{k} & 0 \\ 0 & \frac{-k_y^2-\nu k_x^2}{k^2} & \frac{k_e^2-\nu k_x^2}{k^2} & 0 \end{bmatrix}.$$

Case 3:

$$\mathbf{T}_{11} = \begin{bmatrix} 0 & 0 & \frac{k_x}{k} & -\frac{k_x}{k} \\ 0 & 0 & -\frac{k_{ly}}{k} & -\frac{k_{ly}}{k}\cos\alpha \\ 1 & 1 & 0 & -\frac{k_{ly}}{k}\sin\alpha \\ 0 & 0 & -2\frac{k_x k_{ly}}{k^2} & -2\frac{k_x k_{ly}}{k^2} \end{bmatrix},$$

$$\mathbf{T}_{12} = \begin{bmatrix} 0 & 0 & -\frac{k_{sy}}{k} & -\frac{k_{sy}}{k} \\ \sin\alpha & \sin\alpha & -\frac{k_x}{k} & \frac{k_x}{k}\cos\alpha \\ -\cos\alpha & -\cos\alpha & 0 & \frac{k_x}{k}\sin\alpha \\ 0 & 0 & \frac{(k_{sy}^2-k_x^2)}{k^2} & \frac{(k_x^2-k_{sy}^2)}{k^2} \end{bmatrix},$$

$$\mathbf{T}_{21} = \begin{bmatrix} 0 & 0 & \mathrm{j}\frac{k_{ly}^2+\nu k_x^2}{k^2} & -\mathrm{j}\frac{k_{ly}^2+\nu k_x^2}{k^2}\cos\alpha \\ \mathrm{j}\frac{D(-1+\nu^2)k_y(k_y^2+(2-\nu)k_x^2)}{Ehk} & \frac{D(-1+\nu^2)k_e(k_e^2+(2-\nu)k_x^2)}{Ehk} & 0 & \mathrm{j}\frac{k_{ly}^2+\nu k_x^2}{k^2}\sin\alpha \\ \mathrm{j}\frac{k_y}{k} & \frac{k_e}{k} & 0 & 0 \\ \frac{k_y^2+\nu k_x^2}{k^2} & \frac{-k_e^2+\nu k_x^2}{k^2} & 0 & 0 \end{bmatrix},$$

$$\mathbf{T}_{22} = \begin{bmatrix} \mathrm{j}\frac{D(-1+\nu^2)k_y(k_y^2+(2-\nu)k_x^2)}{Ehk}\sin\alpha & \frac{D(-1+\nu^2)k_e(-k_e^2+(2-\nu)k_x^2)}{Ehk}\sin\alpha & -\mathrm{j}\frac{k_x k_{sy}(\nu-1)}{k^2} & -\mathrm{j}\frac{k_x k_{sy}(\nu-1)}{k^2}\cos\alpha \\ \mathrm{j}\frac{D(-1+\nu^2)k_y(k_y^2+(2-\nu)k_x^2)}{Ehk}\cos\alpha & \frac{D(-1+\nu^2)k_e(-k_e^2+(2-\nu)k_x^2)}{Ehk}\cos\alpha & 0 & -\mathrm{j}\frac{k_x k_{sy}(\nu-1)}{k^2}\sin\alpha \\ 0 & \mathrm{j}\frac{k_y}{k} & \frac{k_e}{k} & 0 \\ 0 & \frac{-k_y^2-\nu k_x^2}{k^2} & \frac{k_e^2-\nu k_x^2}{k^2} & 0 \end{bmatrix},$$

and $\mathbf{b}$ is the term corresponding to incident wave:

$$\mathbf{b} = \begin{bmatrix} 0 \\ 0 \\ -1 \\ 0 \\ 0 \\ \mathrm{j}\frac{D(-1+\nu^2)k_y(k_y^2+(2-\nu)k_x^2)}{Ehk} \\ \mathrm{j}\frac{k_y}{k} \\ \frac{(-k_y^2+\nu k_x^2)}{k^2} \end{bmatrix}.$$

One can easily show that this linear system can be written using only four parameters:, a non-dimensional parameter $\xi = \rho h^2\omega^2/12E$, the Poisson ratio v, connecting angle α and incident angle θ. Expressions of variables used above are

$$\frac{k_x}{k} = \cos\theta,$$

$$\frac{k_y}{k} = \sin\theta,$$

$$\frac{\lambda^4}{k^4} = (1-v^2)\rho\frac{h^2\omega^2}{12E} = (1-v^2)\xi,$$

$$\frac{\mu^4}{k^4} = \frac{4}{(1-v)^2}\frac{\lambda^4}{k^4} = 4\frac{(1+v)}{(1-v)}\xi,$$

$$\frac{k_e^2}{k^2} = 1+\cos^2\theta,$$

$$\frac{k_{ly}^2}{k^2} = \frac{\lambda^2}{k^2} - \frac{k_x^2}{k^2} = \sqrt{(1-v^2)\xi} - \cos^2\theta,$$

$$\frac{k_{sy}^2}{k^2} = \frac{\mu^2}{k^2} - \frac{k_x^2}{k^2} = 2\sqrt{\frac{1+v}{1-v}\xi} - \cos^2\theta,$$

$$\frac{Dk^2}{Eh} = \sqrt{\frac{\xi}{1-v^2}}.$$

Appendix C. In-plane incident wave

The considered incident wave is an in-plane longitudinal one of unit amplitude:

$$u_i = \frac{k_x}{\lambda}\mathrm{e}^{(-\mathrm{j}k_x x - \mathrm{j}k_{ly}y)},$$

$$v_i = \frac{k_{ly}}{\lambda}\mathrm{e}^{(-\mathrm{j}k_x x - \mathrm{j}k_{ly}y)}.$$

Its incidence angle is denoted θ:

$$k_x = \lambda\cos\theta,$$

$$k_{ly} = \lambda\sin\theta,$$

in which λ is the longitudinal wave number: $\lambda^2 = \rho\omega^2(1-v^2)/E$.

Reflected and transmitted in-plane waves are

$$u_r = \mathrm{e}^{-\mathrm{j}k_x x}\left(\frac{k_x}{k} C\mathrm{e}^{\mathrm{j}k_{ly}y} + \frac{k_{sy}}{k} P\mathrm{e}^{\mathrm{j}k_{sy}y}\right),$$

$$v_r = \mathrm{e}^{-\mathrm{j}k_x x}\left(-\frac{k_{ly}}{k} C\mathrm{e}^{\mathrm{j}k_{ly}y} + \frac{k_x}{k} P\mathrm{e}^{\mathrm{j}k_{sy}y}\right),$$

$$u_t = \mathrm{e}^{-\mathrm{j}k_x x}\left(\frac{k_x}{k} F\mathrm{e}^{-\mathrm{j}k_{ly}y} - \frac{k_{sy}}{k} Q\mathrm{e}^{-\mathrm{j}k_{sy}y}\right),$$

$$v_t = \mathrm{e}^{-\mathrm{j}k_x x}\left(\frac{k_{ly}}{k} F\mathrm{e}^{-\mathrm{j}k_{ly}y} + \frac{k_x}{k} Q\mathrm{e}^{-\mathrm{j}k_{sy}y}\right).$$

Considered materials are such that the in-plane shear wave number $\mu = 2(1-\nu)\lambda$ is greater than λ, then all in-plane waves are propagative.

As far as bending waves are concerned, one should distinguish two cases:

- *Case* 1: $k \geqslant k_x$ in which k is the bending wave number: $k^2 = \omega\sqrt{\rho h/D}$.

Thus $k_y = \sqrt{k^2 - k_x^2}$ and $k_e = \sqrt{k + k_x^2}$ correspond to travelling and near-field parts of reflected and transmitted bending waves:

$$w_r = \mathrm{e}^{-\mathrm{j}k_x x}(A\mathrm{e}^{\mathrm{j}k_y y} + B\mathrm{e}^{k_e y}),$$

$$w_t = \mathrm{e}^{-\mathrm{j}k_x x}(H\mathrm{e}^{-\mathrm{j}k_y y} + K\mathrm{e}^{-k_e y}).$$

Linear system obtained using continuity relations along coupling line is denoted $\mathbf{T}.\mathbf{X} = \mathbf{b}$, in which $\mathbf{X}^{\mathrm{t}} = [A\ B\ C\ F\ H\ K\ P\ Q]$, corresponding to waves amplitudes defined above. $\mathbf{T}$ is an (8×8) matrix:

$$\mathbf{T} = \begin{bmatrix} \mathbf{T}_{11} & \mathbf{T}_{12} \\ \mathbf{T}_{21} & \mathbf{T}_{22} \end{bmatrix},$$

$$\mathbf{T}_{11} = \begin{bmatrix} 0 & 0 & \frac{k_x}{\lambda} & -\frac{k_x}{\lambda} \\ 0 & 0 & -\frac{k_{ly}}{\lambda} & -\frac{k_{ly}}{\lambda}\cos\alpha \\ 1 & 1 & 0 & \frac{k_{ly}}{\lambda}\sin\alpha \\ 0 & 0 & 2\frac{k_x k_{ly}}{\lambda k} & 2\frac{k_x k_{ly}}{\lambda k} \end{bmatrix},$$

$$\mathbf{T}_{12} = \begin{bmatrix} 0 & 0 & \frac{k_{sy}}{\lambda} & \frac{k_{sy}}{\lambda} \\ -\sin\alpha & -\sin\alpha & \frac{k_x}{\lambda} & -\frac{k_x}{\lambda}\cos\alpha \\ -\cos\alpha & -\cos\alpha & 0 & \frac{k_x}{\lambda}\sin\alpha \\ 0 & 0 & \frac{(k_{sy}^2 - k_x^2)}{k\lambda} & \frac{(k_x^2 - k_{sy}^2)}{k\lambda} \end{bmatrix},$$

$$\mathbf{T}_{21} = \begin{bmatrix} 0 & 0 & \mathrm{j}\frac{k_{ly}^2+\nu k_x^2}{\lambda k} & -\mathrm{j}\frac{k_{ly}^2+\nu k_x^2}{\lambda k}\cos\alpha \\ \mathrm{j}\frac{Dk_y(k_y^2+(2-\nu)k_x^2)}{Ehk} & \frac{Dk_e(-k_e^2+(2-\nu)k_x^2)}{Ehk} & 0 & \mathrm{j}\frac{k_{ly}^2+\nu k_x^2}{\lambda k(-1+\nu^2)}\sin\alpha \\ \mathrm{j}\frac{k_y}{k} & \frac{k_e}{k} & 0 & 0 \\ k_y^2+\nu k_x^2 & -k_e^2+\nu k_x^2 & 0 & 0 \end{bmatrix},$$

$$\mathbf{T}_{22} = \begin{bmatrix} \mathrm{j}\frac{D(-1+\nu^2)k_y(k_y^2+(2-\nu)k_x^2)}{Ehk}\sin\alpha & \frac{D(-1+\nu^2)k_e(-k_e^2+(2-\nu)k_x^2)}{Ehk}\sin\alpha & \mathrm{j}\frac{k_xk_{sy}(\nu-1)}{k\lambda} & \mathrm{j}\frac{k_xk_{sy}(\nu-1)}{k\lambda}\cos\alpha \\ \mathrm{j}\frac{Dk_y(k_y^2+(2-\nu)k_x^2)}{Ehk}\cos\alpha & \frac{Dk_e(-k_e^2+(2-\nu)k_x^2)}{Ehk}\cos\alpha & 0 & -\mathrm{j}\frac{k_xk_{sy}}{k\lambda(1+\nu)}\sin\alpha \\ \mathrm{j}\frac{k_y}{k} & \frac{k_e}{k} & 0 & 0 \\ -k_y^2-\nu k_x^2 & k_e^2-\nu k_x^2 & 0 & 0 \end{bmatrix},$$

and the vector $\mathbf{b}$ is

$$\mathbf{b} = \begin{bmatrix} -\frac{k_x}{\lambda} \\ -\frac{k_y}{\lambda} \\ 0 \\ 2\frac{k_xk_{ly}}{\lambda k} \\ -\mathrm{j}\frac{(k_{ly}^2+\nu k_x^2)}{k\lambda} \\ 0 \\ 0 \\ 0 \end{bmatrix}.$$

- *Case* 2: $k < k_x$

All bending waves are near field ones, with wave numbers $k_y = \sqrt{k_x^2 - k^2}$ and $k_e = \sqrt{k + k_x^2}$:

$$w_r = \mathrm{e}^{-\mathrm{j}k_xx}(A\mathrm{e}^{k_yy} + B\mathrm{e}^{k_ey}),$$

$$w_t = \mathrm{e}^{-\mathrm{j}k_xx}(H\mathrm{e}^{-k_yy} + K\mathrm{e}^{-k_ey}).$$

Linear system obtained using continuity relations along coupling line is denoted $\mathbf{T}.\mathbf{X} = \mathbf{b}$, in which $\mathbf{X}^{\mathrm{T}} = [A\ B\ C\ F\ H\ K\ P\ Q]$, corresponding to waves amplitudes defined above. $\mathbf{T}$ is a (8×8) matrix:

$$\mathbf{T} = \begin{bmatrix} \mathbf{T}_{11} & \mathbf{T}_{12} \\ \mathbf{T}_{21} & \mathbf{T}_{22} \end{bmatrix}.$$

Components of $\mathbf{T}_{11}$ and $\mathbf{T}_{12}$ are similar to those given in case 1.

$$\mathbf{T}_{21} = \begin{bmatrix} 0 & 0 & \mathrm{j}\frac{(k_{ly}^2+\nu k_x^2)}{\lambda k} & -\mathrm{j}\frac{(k_{ly}^2+\nu k_x^2)}{\lambda k}\cos\alpha \\ \frac{Dk_y(-k_y^2+(2-\nu)k_x^2)}{Ehk} & \frac{Dk_e(-k_e^2+(2-\nu)k_x^2)}{Ehk} & 0 & \mathrm{j}\frac{(k_{ly}^2+\nu k_x^2)}{\lambda k(-1+\nu^2)}\sin\alpha \\ \frac{k_y}{k} & \frac{k_e}{k} & 0 & 0 \\ (-k_y^2+\nu k_x^2) & (-k_e^2+\nu k_x^2) & 0 & 0 \end{bmatrix},$$

$$\mathbf{T}_{22} = \begin{bmatrix} \frac{D(-1+\nu^2)k_y(-k_y^2+(2-\nu)k_x^2)}{Ehk}\sin\alpha & \frac{D(-1+\nu^2)k_e(-k_e^2+(2-\nu)k_x^2)}{Ehk}\sin\alpha & \mathrm{j}\frac{k_xk_{sy}(\nu-1)}{k\lambda} & \mathrm{j}\frac{k_xk_{sy}(\nu-1)}{k\lambda}\cos\alpha \\ \frac{Dk_y(-k_y^2+(2-\nu)k_x^2)}{Ehk}\cos\alpha & \frac{Dk_e(-k_e^2+(2-\nu)k_x^2)}{Ehk}\cos\alpha & 0 & -\mathrm{j}\frac{k_xk_{sy}}{k\lambda(1+\nu)}\sin\alpha \\ \frac{k_y}{k} & \frac{k_e}{k} & 0 & 0 \\ k_y^2-\nu k_x^2 & k_e^2-\nu k_x^2 & 0 & 0 \end{bmatrix}.$$

Appendix D. In-plane shear incident wave

The imposed wave is a travelling in-plane shear one:

$$u_i = -\frac{k_{sy}}{\mu}\mathrm{e}^{-\mathrm{j}k_xx-\mathrm{j}k_{sy}y},$$

$$v_i = \frac{k_x}{\mu}\mathrm{e}^{-\mathrm{j}k_xx-\mathrm{j}k_{sy}y}.$$

Its incidence is denoted θ:

$$k_x = \mu\cos\theta,$$

$$k_{sy} = \mu\sin\theta,$$

in which $\mu^2 = 2\rho\omega^2(1+\nu)/E$; $k^2 = \omega\sqrt{\rho h/D}$ and $k_e = \sqrt{k+k_x^2}$.

Three cases can be distinguished:

- *Case* 1: $k > \lambda \geqslant k_x$

Then $k_y = \sqrt{k^2-k_x^2}$ and $k_{ly} = \sqrt{\lambda^2-k_x^2}$:

Reflected waves are

$$w_r = \mathrm{e}^{-\mathrm{j}k_xx}(A\mathrm{e}^{\mathrm{j}k_yy} + B\mathrm{e}^{k_ey}),$$

$$u_r = \mathrm{e}^{-\mathrm{j}k_xx}\left(\frac{k_x}{k}C\mathrm{e}^{\mathrm{j}k_{ly}y} + \frac{k_{sy}}{k}P\mathrm{e}^{\mathrm{j}k_{sy}y}\right),$$

$$v_r = \mathrm{e}^{-\mathrm{j}k_xx}\left(-\frac{k_{ly}}{k}C\mathrm{e}^{\mathrm{j}k_{ly}y} + \frac{k_x}{k}P\mathrm{e}^{\mathrm{j}k_{sy}y}\right).$$

Transmitted waves are

$$w_t = \mathrm{e}^{-\mathrm{j}k_x x}(H\mathrm{e}^{-\mathrm{j}k_{ty}y} + K\mathrm{e}^{-k_e y}),$$

$$u_t = \mathrm{e}^{-\mathrm{j}k_x x}\left(\frac{k_x}{k}F\mathrm{e}^{-\mathrm{j}k_{ly}y} - \frac{k_{sy}}{k}Q\mathrm{e}^{-\mathrm{j}k_{sy}y}\right),$$

$$v_t = \mathrm{e}^{-\mathrm{j}k_x x}\left(\frac{k_{ly}}{k}F\mathrm{e}^{-\mathrm{j}k_{ly}y} + \frac{k_x}{k}Q\mathrm{e}^{-\mathrm{j}k_{sy}y}\right).$$

All existing waves are travelling ones.

Linear system obtained using continuity relations along coupling line is denoted $\mathbf{T}.\mathbf{X} = \mathbf{b}$, in which $\mathbf{X}^{\mathrm{t}} = [A\ B\ C\ F\ H\ K\ P\ Q]$, corresponding to waves amplitudes defined above. $\mathbf{T}$ is an (8×8) matrix:

$$\mathbf{T} = \begin{bmatrix} \mathbf{T}_{11} & \mathbf{T}_{12} \\ \mathbf{T}_{21} & \mathbf{T}_{22} \end{bmatrix},$$

$$\mathbf{T}_{11} = \begin{bmatrix} 0 & 0 & \frac{k_x}{k} & -\frac{k_x}{k} \\ 0 & 0 & -\frac{k_{ly}}{k} & -\frac{k_{ly}}{k}\cos\alpha \\ 1 & 1 & 0 & \frac{k_{ly}}{k}\sin\alpha \\ 0 & 0 & 2\frac{k_x k_{ly}}{k^2} & 2\frac{k_x k_{ly}}{k^2} \end{bmatrix},$$

$$\mathbf{T}_{12} = \begin{bmatrix} 0 & 0 & \frac{k_{sy}}{k} & \frac{k_{sy}}{k} \\ -\sin\alpha & -\sin\alpha & \frac{k_x}{k} & -\frac{k_x}{k}\cos\alpha \\ -\cos\alpha & -\cos\alpha & 0 & \frac{k_x}{k}\sin\alpha \\ 0 & 0 & \frac{(k_{sy}^2 - k_x^2)}{k^2} & \frac{(k_x^2 - k_{sy}^2)}{k^2} \end{bmatrix},$$

$$\mathbf{T}_{21} = \begin{bmatrix} 0 & 0 & \mathrm{j}\frac{k_{ly}^2 + \nu k_x^2}{k^2} & -\mathrm{j}\frac{k_{ly}^2 + \nu k_x^2}{k^2}\cos\alpha \\ \mathrm{j}\frac{Dk_y(k_y^2 + (2-\nu)k_x^2)}{Ehk} & \frac{Dk_e(-k_e^2 + (2-\nu)k_x^2)}{Ehk} & 0 & \mathrm{j}\frac{k_{ly}^2 + \nu k_x^2}{(-1+\nu^2)}\sin\alpha \\ \mathrm{j}\frac{k_y}{k} & \frac{k_e}{k} & 0 & 0 \\ \frac{k_y^2 + \nu k_x^2}{k^2} & \frac{-k_e^2 + \nu k_x^2}{k^2} & 0 & 0 \end{bmatrix},$$

$$\mathbf{T}_{22} = \begin{bmatrix} \mathrm{j}\frac{D(-1+\nu^2)k_y(k_y^2 + (2-\nu)k_x^2)}{Ehk}\sin\alpha & \frac{D(-1+\nu^2)k_e(-k_e^2 + (2-\nu)k_x^2)}{Ehk}\sin\alpha & \mathrm{j}\frac{k_x k_{sy}(\nu-1)}{k^2} & \mathrm{j}\frac{k_x k_{sy}(\nu-1)}{k^2}\cos\alpha \\ \mathrm{j}\frac{Dk_y(k_y^2 + (2-\nu)k_x^2)}{Ehk}\cos\alpha & \frac{Dk_e(-k_e^2 + (2-\nu)k_x^2)}{Ehk}\cos\alpha & 0 & -\mathrm{j}\frac{k_x k_{sy}}{(1+\nu)k^2}\sin\alpha \\ \mathrm{j}\frac{k_y}{k} & \frac{k_e}{k} & 0 & 0 \\ (-k_y^2 - \nu k_x^2) & (k_e^2 - \nu k_x^2) & 0 & 0 \end{bmatrix},$$

and the vector $\mathbf{b}$ is

$$\mathbf{b} = \begin{bmatrix} \frac{k_{sy}}{\mu} \\ -\frac{k_x}{\mu} \\ 0 \\ \frac{(k_x^2 - k_{sy}^2)}{\mu k} \\ \mathrm{j}\frac{k_{sy}k_x(\nu-1)}{k\mu} \\ 0 \\ 0 \\ 0 \end{bmatrix}.$$

- *Case* 2: $k \geqslant k_x > \lambda$

Then $k_y = \sqrt{k^2 - k_x^2}$ and $k_{ly} = \mathrm{j}\sqrt{k_x^2 - \lambda^2}$:

Reflected waves are

$$w_r = \mathrm{e}^{-\mathrm{j}k_x x}(A\mathrm{e}^{\mathrm{j}k_y y} + B\mathrm{e}^{k_e y}),$$

$$u_r = \mathrm{e}^{-\mathrm{j}k_x x}\left(\frac{k_x}{k} C\mathrm{e}^{-\mathrm{j}k_{ly} y} + \frac{k_{sy}}{k} P\mathrm{e}^{\mathrm{j}k_{sy} y}\right),$$

$$v_r = \mathrm{e}^{-\mathrm{j}k_x x}\left(\frac{k_{ly}}{k} C\mathrm{e}^{-\mathrm{j}k_{ly} y} + \frac{k_x}{k} P\mathrm{e}^{\mathrm{j}k_{sy} y}\right).$$

Transmitted waves are

$$w_t = \mathrm{e}^{-\mathrm{j}k_x x}(H\mathrm{e}^{-\mathrm{j}k_y y} + K\mathrm{e}^{-k_e y}),$$

$$u_t = \mathrm{e}^{-\mathrm{j}k_x x}\left(\frac{k_x}{k} F\mathrm{e}^{\mathrm{j}k_{ly} y} - \frac{k_{sy}}{k} Q\mathrm{e}^{-\mathrm{j}k_{sy} y}\right),$$

$$v_t = \mathrm{e}^{-\mathrm{j}k_x x}\left(-\frac{k_{ly}}{k} F\mathrm{e}^{\mathrm{j}k_{ly} y} + \frac{k_x}{k} Q\mathrm{e}^{-\mathrm{j}k_{sy} y}\right).$$

All waves are travelling ones, except in-plane longitudinal ones.

Linear system obtained using continuity relations along coupling line is denoted $\mathbf{T}.\mathbf{X} = \mathbf{b}$, in which $\mathbf{X}^{\mathrm{t}} = [A\ B\ C\ F\ H\ K\ P\ Q]$, corresponding to waves amplitudes defined above. $\mathbf{T}$ is an (8×8) matrix:

$$\mathbf{T} = \begin{bmatrix} \mathbf{T}_{11} & \mathbf{T}_{12} \\ \mathbf{T}_{21} & \mathbf{T}_{22} \end{bmatrix},$$

$$\mathbf{T}_{11} = \begin{bmatrix} 0 & 0 & \frac{k_x}{k} & -\frac{k_x}{k} \\ 0 & 0 & \frac{k_{ly}}{k} & \frac{k_{ly}}{k}\cos\alpha \\ 1 & 1 & 0 & -\frac{k_{ly}}{k}\sin\alpha \\ 0 & 0 & -2\frac{k_x k_{ly}}{k^2} & -2\frac{k_x k_{ly}}{k^2} \end{bmatrix},$$

$$\mathbf{T}_{12} = \begin{bmatrix} 0 & 0 & \frac{k_{sy}}{k} & \frac{k_{sy}}{k} \\ -\sin\alpha & -\sin\alpha & \frac{k_x}{k} & -\frac{k_x}{k}\cos\alpha \\ -\cos\alpha & -\cos\alpha & 0 & \frac{k_x}{k}\sin\alpha \\ 0 & 0 & \frac{(k_{sy}^2-k_x^2)}{k^2} & \frac{(k_x^2-k_{sy}^2)}{k^2} \end{bmatrix},$$

$$\mathbf{T}_{21} = \begin{bmatrix} 0 & 0 & \mathrm{j}\frac{k_{ly}^2+\nu k_x^2}{k^2} & -\mathrm{j}\frac{k_{ly}^2+\nu k_x^2}{k^2}\cos\alpha \\ \mathrm{j}\frac{Dk_y(k_y^2+(2-\nu)k_x^2)}{Ehk} & \frac{Dk_e(-k_e^2+(2-\nu)k_x^2)}{Ehk} & 0 & \mathrm{j}\frac{k_{ly}^2+\nu k_x^2}{(-1+\nu^2)}\sin\alpha \\ \mathrm{j}\frac{k_y}{k} & \frac{k_e}{k} & 0 & 0 \\ \frac{k_y^2+\nu k_x^2}{k^2} & \frac{-k_e^2+\nu k_x^2}{k^2} & 0 & 0 \end{bmatrix},$$

$$\mathbf{T}_{22} = \begin{bmatrix} \mathrm{j}\frac{D(-1+\nu^2)k_y(k_y^2+(2-\nu)k_x^2)}{Ehk}\sin\alpha & \frac{D(-1+\nu^2)k_e(-k_e^2+(2-\nu)k_x^2)}{Ehk}\sin\alpha & \mathrm{j}\frac{k_x k_{sy}(\nu-1)}{k^2} & \mathrm{j}\frac{k_x k_{sy}(\nu-1)}{k^2}\cos\alpha \\ \mathrm{j}\frac{Dk_y(k_y^2+(2-\nu)k_x^2)}{Ehk}\cos\alpha & \frac{Dk_e(-k_e^2+(2-\nu)k_x^2)}{Ehk}\cos\alpha & 0 & -\mathrm{j}\frac{k_x k_{sy}}{(1+\nu)k^2}\sin\alpha \\ \mathrm{j}\frac{k_y}{k} & \frac{k_e}{k} & 0 & 0 \\ -k_y^2-\nu k_x^2 & k_e^2-\nu k_x^2 & 0 & 0 \end{bmatrix}.$$

- *Case* 3: $k_x > k > \lambda$

Then $k_y = \sqrt{k_x^2 - k^2}$ and $k_{ly} = \mathrm{j}\sqrt{k_x^2 - \lambda^2}$:

Reflected waves are

$$w_r = \mathrm{e}^{-\mathrm{j}k_x x}(A\mathrm{e}^{k_y y} + B\mathrm{e}^{k_e y}),$$

$$u_r = \mathrm{e}^{-\mathrm{j}k_x x}\left(\frac{k_x}{k}C\mathrm{e}^{-\mathrm{j}k_{ly} y} + \frac{k_{sy}}{k}P\mathrm{e}^{\mathrm{j}k_{sy} y}\right),$$

$$v_r = \mathrm{e}^{-\mathrm{j}k_x x}\left(\frac{k_{ly}}{k}C\mathrm{e}^{-\mathrm{j}k_{ly} y} + \frac{k_x}{k}P\mathrm{e}^{\mathrm{j}k_{sy} y}\right).$$

Transmitted waves are

$$w_t = \mathrm{e}^{-\mathrm{j}k_x x}(H\mathrm{e}^{-k_y y} + K\mathrm{e}^{-k_e y}),$$

$$u_t = \mathrm{e}^{-\mathrm{j}k_x x}\left(\frac{k_x}{k}F\mathrm{e}^{\mathrm{j}k_{ly} y} - \frac{k_{sy}}{k}Q\mathrm{e}^{-\mathrm{j}k_{sy} y}\right),$$

$$v_t = \mathrm{e}^{-\mathrm{j}k_x x}\left(-\frac{k_{ly}}{k}F\mathrm{e}^{\mathrm{j}k_{ly}y} + \frac{k_x}{k}Q\,\mathrm{e}^{-\mathrm{j}k_{sy}y}\right).$$

All waves are near-field ones, except in-plane shear ones.

Linear system obtained using continuity relations along coupling line is denoted $\mathbf{T}.\mathbf{X} = \mathbf{b}$, in which $\mathbf{X}^{\mathrm{t}} = [A\ B\ C\ F\ H\ K\ P\ Q]$, corresponding to waves amplitudes defined above. $\mathbf{T}$ is an (8×8) matrix:

$$\mathbf{T} = \begin{bmatrix} \mathbf{T}_{11} & \mathbf{T}_{12} \\ \mathbf{T}_{21} & \mathbf{T}_{22} \end{bmatrix},$$

$$\mathbf{T}_{11} = \begin{bmatrix} 0 & 0 & \frac{k_x}{k} & -\frac{k_x}{k} \\ 0 & 0 & \frac{k_{ly}}{k} & \frac{k_{ly}}{k}\cos\alpha \\ 1 & 1 & 0 & -\frac{k_{ly}}{k}\sin\alpha \\ 0 & 0 & -2\frac{k_x k_{ly}}{k^2} & -2\frac{k_x k_{ly}}{k^2} \end{bmatrix},$$

$$\mathbf{T}_{12} = \begin{bmatrix} 0 & 0 & \frac{k_{sy}}{k} & \frac{k_{sy}}{k} \\ -\sin\alpha & -\sin\alpha & \frac{k_x}{k} & -\frac{k_x}{k}\cos\alpha \\ -\cos\alpha & -\cos\alpha & 0 & \frac{k_x}{k}\sin\alpha \\ 0 & 0 & \frac{(k_{sy}^2-k_x^2)}{k^2} & \frac{(k_x^2-k_{sy}^2)}{k^2} \end{bmatrix},$$

$$\mathbf{T}_{21} = \begin{bmatrix} 0 & 0 & \mathrm{j}\frac{k_{ly}^2+\nu k_x^2}{k^2} & -\mathrm{j}\frac{k_{ly}^2+\nu k_x^2}{k^2}\cos\alpha \\ \frac{Dk_y(-k_y^2+(2-\nu)k_x^2)}{Ehk} & \frac{Dk_e(-k_e^2+(2-\nu)k_x^2)}{Ehk} & 0 & \mathrm{j}\frac{k_{ly}^2+\nu k_x^2}{(-1+\nu^2)}\sin\alpha \\ \frac{k_y}{k} & \frac{k_e}{k} & 0 & 0 \\ \frac{-k_y^2+\nu k_x^2}{k^2} & \frac{-k_e^2+\nu k_x^2}{k^2} & 0 & 0 \end{bmatrix},$$

$$\mathbf{T}_{22} = \begin{bmatrix} \frac{D(-1+\nu^2)k_y(-k_y^2+(2-\nu)k_x^2)}{Ehk}\sin\alpha & \frac{D(-1+\nu^2)k_e(-k_e^2+(2-\nu)k_x^2)}{Ehk}\sin\alpha & \mathrm{j}\frac{k_x k_{sy}(\nu-1)}{k^2} & \mathrm{j}\frac{k_x k_{sy}(\nu-1)}{k^2}\cos\alpha \\ \frac{Dk_y(-k_y^2+(2-\nu)k_x^2)}{Ehk}\cos\alpha & \frac{Dk_e(-k_e^2+(2-\nu)k_x^2)}{Ehk}\cos\alpha & 0 & -\mathrm{j}\frac{k_x k_{sy}}{(1+\nu)k^2}\sin\alpha \\ \frac{k_y}{k} & \frac{k_e}{k} & 0 & 0 \\ k_y^2 - \nu k_x^2 & k_e^2 - \nu k_x^2 & 0 & 0 \end{bmatrix}.$$

Appendix E. Notations for Section 2

$(O, \vec{x_1})$	neutral axis of beam 1
$\vec{y_1}$	flexural axis of beam 1
$(O, \vec{x_2})$	neutral axis of beam 2
$\vec{y_2}$	flexural axis of beam 2

$(O,\vec{z})$	common normal axis to $(O,\vec{x_1},\vec{y_1})$ and $(O,\vec{x_2},\vec{y_2})$ planes
α	coupling angle
w_1	flexural displacement of beam 1
w_2	flexural displacement of beam 2
k	flexural wave number
ω	frequency of excitation (rad/s)
S	beams sections
E	Young's modulus
I	moment of inertia of the beam
u_1	longitudinal displacement of beam 1
u_2	longitudinal displacement of beam 2
λ	longitudinal wave number
ρ	density
M	bending moment
T	shear force
N	longitudinal force
Ω	rotation of the beam cross-section
μ	wave number ratio
f	frequency of excitation (Hz)
P_T	power transmitted by shear force
P_M	power transmitted by bending moment
$P_{bending}$	power transmitted by bending movement
P_{longi}	power transmitted by longitudinal movement
P_{trans}	total transmitted power
P_{inc}	incident power
P_{refl}	reflected power
α_{crit}	critical angle value
L_i	length of beam i

Appendix F. Notations for Section 3

$\vec{x}$	coupling line axis
$(\vec{x},\vec{y_0})$	first plate plane
$\vec{z_0}$	normal axis to plate 1
$(\vec{x},\vec{y_1})$	second plate plane
$\vec{z_1}$	normal axis to plate 2
α	coupling angle
θ	incident angle of exciting wave
u, v and w	displacement components
k	flexural wave number
ω	frequency (rad/s)
ρ	density of material
E	Young's modulus of material

h	common thickness of plates
D	flexural rigidity of plates: $D = Eh^3/12(1-v^2)$
v	the Poisson ratio of material
λ	in-plane longitudinal wave number
μ	in-plane shear wave number
ξ	non-dimensional parameter $\xi = \rho h^2\omega^2/12E$

References

[1] E. Blain, D. Aubry, P. Chove, P. Lardeur, Influence of parameters dispersion on the vibrating behaviour of spot welded plates, in: P. Level, T. Tison, B. Lallemand, G. Plessis (Eds.), Euromech 405: Numerical Modelling Of Uncertainties, Valenciennes, November 1999, Presses Universitaires de Valenciennes, Valenciennes, 1999.

[2] R. Bernhard, The limits of predictability due to manufacturing and environmentally induced uncertainty, in: F.A. Hill, R. Lawrence (Eds.), Inter-Noise 96, Liverpool, Institute of Acoustics, St. Albens, 1996.

[3] M. Ouisse, J.-L. Guyader, Localization of structural zones producing hypersensitive behavior, in: L. Cheng, K.M. Li, R.M.C. Lo (Eds.), Proceedings of the Eighth International Congress on Sound and Vibration, Hong Kong, July 2001, Hong Kong Polytechnic University, Hong Kong.

[4] E. Rébillard, J. Guyader, Vibrational behaviour of lattices of plates: basic behaviour and hypersensitivity phenomena, Journal of Sound and Vibration 205 (3) (1997) 337–354.

[5] E. Rébillard, J. Guyader, Vibrational behaviour of a population of coupled plates: hypersensitivity to the connexion angle, Journal of Sound and Vibration 188 (3) (1995) 435–454.

[6] J. Horner, R. White, Prediction of vibrational power transmission through bends and joints in beam-like structures, Journal of Sound and Vibration 147 (1) (1991) 87–103.

[7] Y. Guo, Flexural wave transmission through angled structural joints, Journal of the Acoustical Society of America 97 (1) (1997) 289–297.

[8] R. Langley, K. Heron, Elastic wave transmission through plate/beam junctions, Journal of Sound and Vibration 143 (2) (1990) 241–253.

[9] H.-G. Kil, D.-H. Park, S.-Y. Hong, J.-J. Jeon, Power flow models and analysis of in-plane waves in finite coupled thin plates, Journal of Sound and Vibration 244 (4) (2001) 651–668.